Student Final Report No. 7784 **January 2017**

The use of computed tomography based predictors of meat quality in sheep breeding programmes

January 2017

Student Final Report No. 7784

The use of computed tomography based predictors of meat quality in sheep breeding programmes

Neil Clelland

SRUC

Roslin Institute Building

Midlothian

Edinburgh

EH25 9RG

Supervisors: Dr Nicola Lambe (SRUC); Prof Lutz Bünger (SRUC) and Dr Sara Knott (University of Edinburgh)

This is the final report of a PhD project (AHDB Beef and Lamb Ref: 7784) that ran from November 2011 to November 2015. The work was funded by AHDB Beef and Lamb, HCC and QMS.

AHDB Beef and Lamb is the beef and lamb division of the Agriculture and Horticulture Development Board for levy payers in England.

Hybu Cig Cymru - Meat Promotion Wales (HCC) is the Welsh red meat organisation for levy payers in Wales.

Quality Meat Scotland (QMS) is the Scottish red meat organisation for levy payers in Scotland.

CONTENTS

List of Abbreviations

Abbreviation	Explanation
AHDB	Agriculture and horticulture development board
ANOVA	Analysis of variance
AOAC	Association of analytical communities
BioSS	Bio-informatics and Statistics Scotland
Chem_IMF	Chemically extracted intramuscular fat
CT	X-ray computed tomography
CT_Age	Age at X-ray computed tomography scanning
CTLWT	Live weight at CT scanning
CTMD	Computed tomography muscle density
EBLEX	English Beef and Lamb Executive
EU	European Union
FD	Fat density
FSD	Standard deviation of fat density
f_vol	Fat tissue volume
HU	Hounsfield unit
IMF	Intramuscular Fat
ISC	Ischium
ISCFA	Fat area in the ischium region
ISCFD	Average fat density in the ischium region
ISCFSD	Standard deviation of fat density in the ischium region
ISCMA	Muscle area in the ischium region
ISCMD	Average muscle density in the ischium region
ISCMSD	Standard deviation of muscle density in the ischium region
ISCSTD	Average soft tissue density in the ischium region
ISCSTSD	Standard deviation of soft tissue density in the ischium region
KgF	Kilogrammes of force
LV5	5^{th} lumbar vertebra
LV5FA	Fat area in the 5^{th} lumbar vertebra region
LV5FD	Average fat density in the 5^{th} lumbar vertebra region
LV5FSD	Standard deviation of fat density in the 5^{th} lumbar vertebra region
LV5MA	Muscle area in the 5^{th} lumbar vertebra region
LV5MD	Average muscle density in the 5^{th} lumbar vertebra region
LV5MSD	Standard deviation of muscle density in the 5^{th} lumbar vertebra region
LV5STD	Average soft tissue density in the 5^{th} lumbar vertebra region
LV5STSD	Standard deviation of soft tissue density in the 5^{th} lumbar vertebra region
LW	Live weight
MD	Muscle density
MEQ	Meat eating quality
MSD	Standard deviation of muscle density
MQ	Meat quality
OLS	Ordinary least squares
PLS	Partial least squares

Abbreviation	Explanation
Pr_Cfat	Computed tomography predicted carcass fat
Pr_IMF	X-ray computed tomography predicted intramuscular fat
RMSE	Residual mean square error
RMSEP	Residual mean square error of prediction
ROI	Region of interest
SBF	Scottish blackface sheep
SCTS	Spiral computed tomography scanning
SD	Standard deviation
ShF	Mechanical shear-force
SL_Age	Age at slaughter
SRUC	Scotland's rural college
STAR	Sheep tomogram analysis routines
STD	Soft tissue density
STSD	Standard deviation of soft tissue density
Tex	Texel sheep
TexX	Texel crossed with Mule sheep
TV8	8^{th} thoracic vertebra
TV8FA	Fat area in the 8^{th} thoracic vertebra
TV8FD	Average fat density in the 8^{th} thoracic vertebra region
TV8FSD	Standard deviation of fat density in the 8^{th} thoracic vertebra region
TV8MA	Muscle area in the 8^{th} thoracic vertebra
TV8MD	Average muscle density in the 8^{th} thoracic vertebra
TV8MSD	Standard deviation of muscle density in the 8th thoracic vertebra region
TV8STD	Average soft tissue density in the 8^{th} thoracic vertebra region
TV8STSD	Standard deviation of soft tissue density in the 8^{th} thoracic vertebra region
UK	United Kingdom
US	Ultrasound
w_fd	Weighted average fat density
w_fsd	Weighted standard deviation of fat density
w_md	Weighted average muscle density
w_msd	Weighted standard deviation of muscle density
w_std	Weighted average soft tissue density
w_stsd	Weighted standard deviation of soft tissue density
m_vol	Muscle tissue volume

1. Abstract

One of the main drivers influencing consumers in the purchasing of red meat is the level of visible fat, and this is particularly important in lamb, as lamb often perceived as fatty. Consumer-driven preference for leaner meat coupled with the meat processing industries preference for a reduction in carcass fat, increasing lean meat yield and reducing waste, have led to continued selection for increased lean and reduced fatness in several meat producing species. The perception of lamb being fatty could be directly targeted in isolation by reducing overall fat levels, however there are related effects to meat (eating) quality, and the combined improvement and consistency of meat (eating) quality and the reduction of overall fatness is more complicated.

It is apparent that fat content of meat plays a significant role in (eating) quality. Generally four major fat depots are recognised in animal carcasses, these are: subcutaneous (under the skin); internal organ associated; intermuscular (between muscles and surrounding muscle groups); and intramuscular (marbling, between muscle fibres), the latter is generally regarded as having the greatest association with meat (eating) quality.

X-ray computed tomography (CT) can measure the volume of the main body tissues fat, muscle and bone in live sheep with very high accuracy and CT predictions of carcass composition have been used in commercial UK sheep breeding programmes over the last two decades. Together with ultrasound measures of fat and muscle depth in the loin region, CT measured carcass fat and muscle weights have contributed much to the success of breeding for leaner carcasses and increased lean meat yield. Recently it has also been considered that CT provides the means to simultaneously estimate intramuscular fat (IMF or marbling) and carcass fat *in vivo*.

Thus the aim of this project is to investigate the use of two and three-dimensional CT techniques in the estimation of meat (eating) quality traits in sheep, and to further investigate the genetic basis of these traits and the possibility of their inclusion into current breeding programmes. The primary approach was the use of two-dimensional CT, determining the most accurate combination of variables to predict intramuscular fat and tenderness in the loin. The prediction of tenderness was poor with accuracies ranging from 3% to 14% (100% accuracy being the best). However the prediction of marbling in the loin was more promising. Simple single CT variables, obtained during routine CT scanning, predicted marbling with around 51% accuracy. These accuracies were significantly improved upon by including additional information from the CT scans, which increased the accuracy to more than 65%. Similar results were achieved with the use of information from three-dimensional CT

scanning techniques (51% – 71% accuracy), however, there was a dramatically increased requirement for image analysis associated with higher labour costs when compared to predictions based on two-dimensional techniques. In addition, the increase in accuracy was not significant and therefore the increased labour input not justified. This suggests that the current method of two-dimensional image capture is providing sufficiently informative predictors for the accurate estimation of intramuscular fat in live sheep. This is important as the selection trait can be directly on selection candidates providing higher accuracies than sib testing.

The prediction equations developed as part of this work were applied across divergent breeds (Texel, Scottish Blackface and Texel cross Scotch Mule), to investigate the transferability of the prediction equations directly across to other breeds of sheep.

Using the models previously developed in purebred Texel to predict intramuscular fat in the Scottish Blackface and Texel cross mule, accuracies were found to be 57% – 64% in Scottish Blackface and 37% – 38% in Texel cross Mule, providing evidence that the equations are transferable across some breeds more successfully than others. However, given that there is currently no method of accurately estimating intramuscular fat (or other meat quality traits) in live sheep, accuracies across both breeds are acceptable.

One part of this study was also to compare the intramuscular fat content across the breed types and sexes. It has been found that intramuscular fat was significantly different across breeds with Scottish Blackface lambs having higher levels of intramuscular fat when compared to Texel cross mule lambs, and the lowest levels of intramuscular fat were in the purebred Texel. Sex also had a significant effect on intramuscular fat in the different breeds with females having higher levels of intramuscular fat. Within the same breed, females had significantly higher levels of intramuscular fat in both the purebred Texel and Scottish Blackface lambs.

The results from this study show that not only is it possible to accurately estimate intramuscular fat in the loin of Texel sheep using CT, but also that the methods developed in this study are transferable across different breed types. The results also show that intramuscular fat predicted by CT is clearly heritable, partially independent of overall fatness and has the potential to be included in current breeding programmes. These findings can now be used to develop breeding programmes enabling breeders to make the best use of modern technology to improve carcass quality whilst simultaneously at least maintaining or possibly even improving aspects of meat (eating) quality using corresponding weighing factors in the index construction.

2. Industry messages

CT scanning allows simultaneous genetic selection for leaner carcasses, whilst maintaining or even increasing intramuscular fat in sheep. This improves simultaneously carcass quality and meat eating quality.

Intramuscular fat could be included in current breeding programmes using current CT scanning protocols and image analysis with minimal additional expense.

Estimated genetic correlations indicate that this is unlikely to affect current breeding goals.

The inclusion of estimated intramuscular fat in current CT scanning procedures and genetic evaluations, provide the potential to simultaneously select animals for carcass leanness and optimal eating quality.

This study provides the required genetic parameters for the UK national genetic evaluation centre (EGENES) to implement these traits into the existing breeding programmes for terminal sire breeds.

3. Introduction

One of the main drivers influencing the decisions made by consumers at point of purchase with regards to red meat, as highlighted by the English beef and lamb executive (EBLEX) report (Allen, 2010), is the level of visible fat associated with lamb. This report highlights that lamb is often perceived as fatty by the consumer. The perception of lamb being fatty could be directly targeted in isolation, however the combined improvement and consistency of meat quality (MQ) and associated meat eating quality (MEQ) characteristics alongside the reduction of overall fatness is more complicated and should be considered in future breeding programmes.

The main quality attributes of meat can be determined in different ways. Measurements of MQ usually describe technological or mechanical factors, such as shear-force (SF), colour, or chemical and toxicological information (e.g. fatty acid profiles, chemically extracted fat content, levels of bacteria, pH etc.), whilst MEQ describes quality attributes concerned with the consumption of fresh meat products relating to organoleptic traits, considering properties such as flavour, tenderness and juiciness. This can only be directly evaluated by a taste panel, but there are proxy methods to predict it, which all need to be calibrated against taste panel results in the first place to quantify accuracy and precision.

In different livestock species, MEQ traits such as flavour, tenderness and juiciness are known to be linked to fat levels (Fernandez et al., 1999; Killinger et al., 2004; Bass et al., 2008). It is apparent that the fat content of meat plays a significant role in the acceptability of major MEQ attributes concerning the consumer and for many decades the influence of fat content on the eating quality of meat has been debated. Generally four major fat depots are recognised in animal carcasses: subcutaneous (under the skin); internal organ-associated (visceral fat, also known as intra-abdominal or organ fat; composed of several adipose depots including mesenteric, epididymal white adipose tissue and perirenal fat); intermuscular (between muscles and surrounding muscle groups); and intramuscular fat (IMF, interspersed within skeletal muscle and between muscle fibres), the latter having the greatest association with MEQ (Fernandez et al., 1999; Killinger et al., 2004).

Consumer-driven preference for leaner meat, coupled with the meat processing industries preference for a reduction in carcass fat, increasing lean meat yield and reducing waste, have led to continued selection for lean growth and reduced fatness in several meat producing species (Sonesson et al., 1998; Simm et al., 2002). However, IMF and back fat thickness are genetically positively correlated in this meat producing species which has resulted in a decrease in IMF content in pigs through genetic selection for decreased back fat which has in turn had a negative effect on the palatability of fresh pork meat (Sonesson et al., 1998). The genetic correlations between meat quality traits and carcass composition have also been investigated in sheep; e.g. Lorentzen and Vangen (2012), reporting a moderately high genetic correlation between IMF and dissected fat (kg). Some studies have reported the negative impact on eating quality when selecting for leaner carcasses in the Australian sheep industry (Lorentzen and Vangen, 2012; Pannier et al., 2014).

Given the genetic relationship between IMF and carcass fat and the possible impact on MEQ previously mentioned, it has been recognised that there is a need to have independent estimates for carcass fat and IMF enabling selection against this positive correlation. Any such divergent selection would not be possible, or at the very least difficult, if the genetic correlation was as a result of pleiotropic genes or tight gene linkage. However, there is evidence that different fat depots are at least partially controlled by different genes in both mice and pigs (Gerbens et al., 1999; Bunger and Hill, 2005).

X-ray computed tomography (CT) can measure fat, muscle and bone *in vivo* in sheep with high accuracy and precision (R^2 values reach mostly 0.95 for muscle and fat) and CT predictions of carcass composition have been used in commercial UK sheep breeding programmes since 2000, following experimental research over the last two decades (Bünger

et al., 2011). Together with ultrasound measures of fat and muscle depth in the loin region, CT measured carcass fat and muscle weights have contributed much to the success of breeding for leaner carcasses and increased lean meat yield (Lewis and Simm, 2002; Jopson et al., 2004). However, previous research has not only demonstrated that CT can estimate carcass fat, but it also provides measurements of the average CT muscle density, which is a good predictor of IMF. Strong negative correlations were found between IMF and CT muscle density in different sheep breeds (Young et al., 2001; Karamichou et al., 2006; Navajas et al., 2008). Taste panel scores for MEQ traits such as flavour, juiciness and overall palatability were also shown to have strong negative genetic and phenotypic correlations with CT muscle density (Karamichou et al., 2007). Advances in CT technology have provided the ability to perform spiral CT scanning, improving the quality and amount of detailed images available through CT, in contrast with earlier 'step and shoot' techniques which involved taking a 'slice' of an area of interest and then moving on to the next area of interest. The use of spiral CT, which is able to capture detailed three-dimensional information, may allow further advances in predicting aspects of meat quality. CT provides the means to quantify simultaneously and independently both IMF and carcass fat *in vivo* enabling these estimates to be exploited in selection programmes simultaneously choosing breeding animals with low carcass fat alongside optimum levels of IMF.

4. Materials and methods

All procedures involving animals were approved by an animal ethics committee at Scotland's Rural College (SRUC) and were performed under United Kingdom Home Office licence following the regulations of the Animals (Scientific Procedures) Act 1986.

4.1. Experimental animals

Data from Texel lambs were available from two previously published studies, these included CT measurements on live lambs pre-slaughter, as well as *post-mortem* laboratory measurements of IMF and shear-force data. The first experiment (Exp 1) was conducted over two years (2003-2004) (Lambe et al., 2008). The second experiment (Exp 2) was conducted in 2009 which included data from two research farms, in Scotland and Wales, where different CT scanners were used for measurements (Lambe et al., 2010a). In the present study, only the data from the research farm in Scotland were used, to reduce possible CT-scanner effects resulting from differences in density value distributions across different scanners. Both Texel data sets were combined to produce one larger data set (Exp 1&2; n=370 across the 2 experiments) consisting of the results from the two separate trials over three separate years.

Data from Scottish Blackface (n=233) lambs were collected as part of the same trial as for the Texels in 2003 and 2004. Data from Texel cross Mule lambs (n=168) were collected as part of a separate historical trial conducted in 2006.

Texel lambs were reared to weaning as either singles (n=184), or twins (n=168), or artificially hand reared (n=25), and consisted of both female and entire male lambs. Scottish Blackface lambs were reared to weaning as either singles (n=106), twins (n=124), or artificially hand reared (n=3), and comprised of females and entire males. Texel cross Mule lambs were reared to weaning as either singles (n=29) or twins (n=137) or unknown litter size (n=2) and comprised of females and castrated males.

All lambs were grazed on low-ground pastures, with the Texel and Scottish Blackface lambs included in the 2003-2004 trial finished with condition score and live weight used as indicators of readiness for slaughter. The remaining Texel (2009) and Texel cross (2006) lambs were reared to an average age of approximately 20 weeks of age and slaughtered as one batch per experiment.

Details of animals used in the study, including within genotype statistics of sex, live weight, slaughter weight CT carcass fat weight and IMF% can be found in Table 4.1. Measured CT traits, liveweight at CT, and slaughter traits (chemically-extracted IMF and age at slaughter) and their acronyms can be found in table 4.2.

Table 4.1: Trait descriptions, means and standard deviations (SD) in Purebred Texel (Tex), Scottish Blackface (SBF) and Texel cross Mule (TexX) lambs, within sex

		Tex Male(n=171) Female(n=199)			**SBF** Male(n=127) Female(n=103)			**TexX** Male(n=82) Female(n=83)		
	Trait Description	Mean	Min-max	SD	Mean	Min-max	SD	Mean	Min-max	SD
CTLWT	Live weight at time of CT scanning									
	Male (Castrates in TexX)	36.2	20.6-49	5.18	35.3	29.8-43.6	3.23	40.3	28.6-51.6	4.88
	Female	34.6	22.3-45.1	4.45	33.2	28.1-38.5	2.62	38.9	23.8-49.8	4.33
CT_Age	Age at CT									
	Male (Castrates in TexX)	131	93-202	20.5	141	105-202	22.9	144	132-151	4.3
	Female	133	95-196	21.43	149	109-202	24.3	143	133-152	4.9
Pr_Cfat	CT Predicted total carcass fat weight (kg)									
	Male (Castrates in TexX)	2.1	0-4.8	0.95	2.7	1.2-5.9	0.92	3.3	0.8-7.1	1.16
	Female	2.6	0.3-6.9	1.20	3.3	1.6-5.8	1.01	3.8	0.4-7.3	1.2
Pr_IMF_A	*M. longissimus lumborum* CT predicted extracted intra-muscular fat (%)									
	Male (Castrates in TexX)	1.31	0.2-2.7	0.49	2.0	1.1-2.9	0.38	1.9	0.7-2.9	0.48
	Female	1.63	0.04-3.3	0.57	2.4	1.4-3.5	0.43	2.2	0.4-3.5	0.47
Pr_IMF_B	*M. longissimus lumborum* CT predicted extracted intra-muscular fat (%)									
	Male (Castrates in TexX)	1.25	0.2-2.5	0.42	2.3	1.0-4.2	0.58	2.1	0.9-4.4	0.61
	Female	1.68	0.1-4.1	0.59	3.1	1.7-4.9	0.75	2.5	0.7-4.8	0.69
Chem_IMF	*M. longissimus lumborum* chemically extracted intra-muscular fat (%)									
	Male (Castrates in TexX)	1.25	0.3-3.7	0.59	2.1	0.2-4.4	0.79	2.1	0.8-3.9	0.62
	Female	1.68	0.4-3.9	0.70	2.5	0.4-4.6	0.79	2.2	0.7-3.8	0.59
SL_Age	Age at slaughter									
	Male (Castrates in TexX)	149	109-234	22.8	158	114-229	25.7	149	139-156	4.15
	Female	150	99-228	23.8	168	113-230	27.9	149	139-157	4.9

Table 4.2: Trait descriptions, means and standard deviations (SD) in Purebred Texel (Tex), Scottish Blackface (SBF) and Texel cross Mule (TexX) lambs

		Tex (n=370)			**SBF** (n=230)			**TexX** (n=165)		
	Trait Description	Mean	Min-max	SD	Mean	Min-max	SD	Mean	Min-max	SD
CT Traits										
CTLWT	Live weight at time of CT scanning	35.35	20.6-49	4.87	34.36	28.1-43.6	3.14	39.62	23.8-51.6	4.64
CT_Age	Age at CT	133	93-202	21.01	145	105-202	23.86	144	132-152	4.62
LV5MD	Average muscle density in 2D scan at the 5th lumbar vertebra (HU)	48.30	41.8-55.9	2.65	44.68	38.7-50.3	2.11	46.45	41.2-53.2	2.06
TV8MD	Average muscle density in 2D scan at the 8th thoracic vertebra (HU)	44.68	36.5-54.7	2.98	39.90	32.2-51.1	2.53	41.99	37.3-51.4	2.37
LV5STD	Average soft tissue density in 2D scan at the 5th lumbar vertebra (HU)	36.22	-1.6-49.5	8.09	18.91	-14.4-44.6	12.27	22.62	-15.6-46.5	11.14
TV8STD	Average soft tissue density in 2D scan at the 8th thoracic vertebra (HU)	21.84	-21.1-46.2	11.35	2.54	-26.6-33.9	12.07	5.41	-27.7-34.4	12.34
ISCSTSD	SD of soft tissue density in 2D scan at the ischium (HU)	40.34	29.3-57.9	5.66	49.40	33.9-66.4	6.02	49.04	34.8-60.9	5.58
LV5STSD	SD of soft tissue density in 2D scan at the 5th lumbar vertebra (HU)	40.33	30.4-64.7	6.19	51.46	31.3-69.1	8.09	51.27	-15.6-46.5	8.44
TV8STSD	SD of soft tissue density in 2D scan at the 8th thoracic vertebra (HU)	50.56	34.1-68.1	6.70	58.01	41.6-68.8	5.49	59.34	42.5-71.9	6.40
Pr_Cfat	CT Predicted total carcass fat weight (kg)	2.34	0-6.9	1.11	3.01	1.2-5.9	1.00	3.54	0.4-7.3	1.21
Pr_IMF_A	*M. longissimus lumborum* CT predicted extracted intra-muscular fat (%)	1.48	0.04-3.3	0.56	2.19	1.1-3.5	0.44	2.07	0.4-3.5	0.48
Pr_IMF_B	*M. longissimus lumborum* CT predicted extracted intra-muscular fat (%)	1.48	0.1-4.1	0.56	2.64	1-4.9	0.77	2.29	0.7-4.8	0.68
Slaughter Traits										
Chem_IMF	*M. longissimus lumborum* chemically extracted intra-muscular fat (%)	1.48	0.3-3.9	0.68	2.28	0.2-4.6	0.82	2.14	0.7-3.9	0.61
SL_Age	Age at slaughter	150	99-234	23.3	163	113-230	27.16	149	139-157	4.56

4.2. Slaughter and meat quality measurements

The majority of lambs finished were slaughtered 4-8 days after CT-scanning, the remaining lambs (n=40 Purebred Texel) were slaughtered 32-33 days after CT scanning, to allow for taste panel analysis after a 30 day withdrawal period from the CT sedative, which formed part of a wider study. Carcasses were chilled for 7 to 9 days and dissected removing the loin muscles from the right side of the carcass, which were vacuum-packed, aged for 7 days and frozen. Carcasses included in Exp 2 were subjected to high voltage electrical stimulation at 700 volts RMS for 45 seconds applied between the end of the processing line and the chill.

Chemical IMF was measured in a cross-sectional sample taken from the top end of the loin (at the first lumbar vertebra). Each sample was blended to a fine paste and chemical IMF percentage was measured as described by Teye et al., (2006).

Shear-force was measured using a standard compression method to determine tenderness simulating the action of the incisor tooth (Volodkevich, 1938). Loins were cooked 'sous-vide' (in-vacuum-packs) in a water bath at 80^{o}C to an internal core temperature of 78^{o}C (Teye et al., 2006), monitoring individual loin temperature using a digital temperature probe (Hanna Instruments, UK). Samples were then immediately cooled in iced water and held at 4^{o}C overnight for a minimum period of 12 hours. Ten samples were taken across the entire loin following the direction of the muscle fibres and tested. Shear-force was recorded as the force required (kgF) to shear the sample, with greater values for less tender samples. Results were averaged over the ten samples taken from each loin.

4.3. In vivo prediction of intramuscular fat content and shear-force in Texel lamb loins using x-ray computed tomography

4.3.1. X-ray computed tomography measurements

Two-dimensional (2D) cross-sectional scans were taken at 3 defined anatomical positions, through the top of the leg at the ischium bone (*i*: ISC), the loin at the fifth lumbar vertebra (*ii*: LV5), and through the chest at the 8th thoracic vertebra (*iii*: *TV8*) (Figure 4.1).

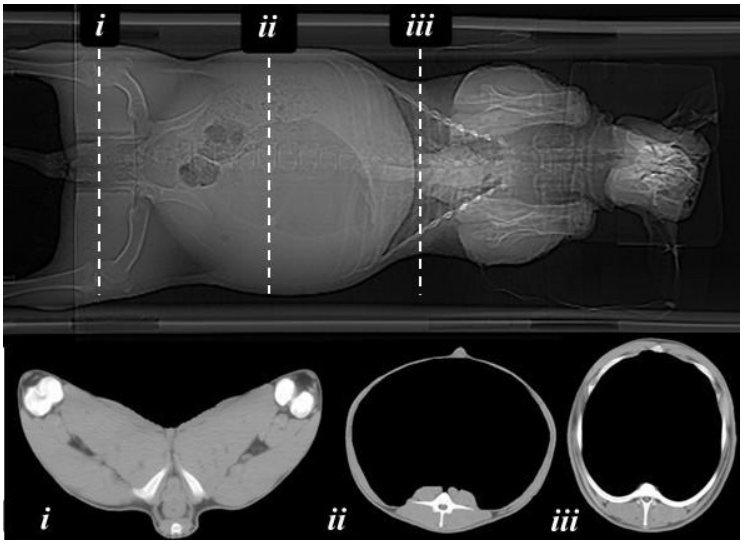

Figure 4.1 Topogram and 2-dimensional cross-sectional CT scans taken in Texel sheep at the ischium (i), 5th lumbar vertebra (ii) and 8th thoracic vertebra (iii)

Image analyses were performed to separate carcass from non-carcass tissues (Glasbey and Young, 2002) and the density of each pixel in the carcass portion was allocated to fat, muscle or bone, according to density thresholds using sheep tomogram analysis routines (STAR) software developed by SRUC and BioSS.

Initial analyses included CT data from all three reference scans. Further analyses were then performed identifying a region of interest (ROI) relating to the anatomical position from where the chemically-extracted IMF and mechanical shear-force was measured (*M. Longissimus lumborum*) from a subsample of animals in the dataset. This involved three levels of image analysis: (*i*) identifying the LV5 scan as the ROI; (*ii*) performing 'virtual dissection' of the LV5 image to isolate the ROI to the muscles surrounding the spine, including *M. longissimus, M. psoas major* and *M. psoas minor*; (*iii*) performing virtual dissection of the LV5 image with the ROI restricted to the right side *M. longissimus* muscle (left side of the image, Figure 4.2)

Carcass fat, as a measure of subcutaneous and intermuscular fat, was also predicted using a breed-specific prediction equation (Texel) developed from previous research (Macfarlane et al., 2006).

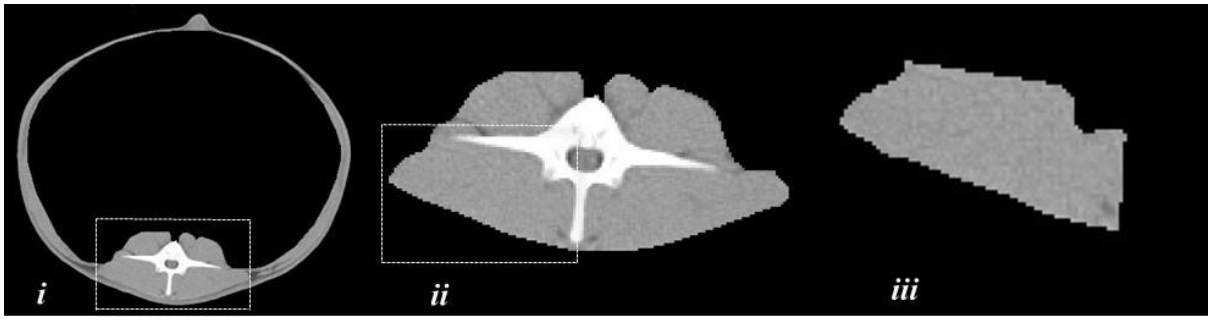

Figure 4.2 Virtual dissections of LV5 scan, LV5 only *(i),* Dissect1 *(ii)* and Dissect2 *(iii)*

4.3.2. Models inclusive of CT estimated carcass fat

CT variables tested in the models to explain variation in IMF and shear-force included Pr_Cfat, as well as measurements from the segmented carcass portions of the three CT reference scan sites (ISC, LV5 and TV8; Figure 4.1): muscle area (MA); fat area (FA); average muscle density (MD); average fat density (FD); standard deviation of muscle density (MSD); standard deviation of fat density (FSD); average soft tissue density (STD); and the standard deviation of soft tissue density (STSD).

Phenotypic correlations amongst CT variables and chemically extracted IMF and shear-force in the loin were calculated to identify linear relationships between variables. Given the strong phenotypic relationship between Pr_Cfat and IMF, Pr_Cfat was fitted as a prefix linear variable (indicative for a 'base line' predictor) in all IMF and shear-force models.

Subsequent models added CT measurement traits in a progressive manner. Firstly, CT variables from all three cross-sectional scan images, including the novel 'soft tissue' calculation (combining the density ranges between fat and muscle), were used to produce prediction equations for IMF and shear-force. Following this, information from the LV5 scan only was used.

To further investigate whether prediction accuracies of IMF could be improved by focusing on the areas of the CT images from which chemical IMF and shear-force was actually measured, a virtual sampling method (segmenting regions of interest from the CT images; Figure 4.2) was then considered (IMF only). This involved a random selection of a subset of animals from Exp 1 (n=100 from year 2003). Mean IMF was 1.77% (SD = 0.72), ranging from 0.42 to 3.75%.

Sixteen models were tested in the analysis. Models using reference data with more than two variables were analysed using stepwise linear regression (Genstat 14^{TM}) to optimize the

combination of predictor variables from the maximum model. Models with one or two variables included were analysed using simple or multiple linear regressions, respectively.

4.3.3. Models independent of CT estimated carcass fat

CT variables were tested in the models to explain IMF only, excluding the use of Pr_Cfat. Muscle density (MD) was considered indicative for a base line predictor for several reasons: a strong phenotypic relationship between muscle density at the 5th lumbar vertebra (LV5MD) and chemically extracted IMF (r = -0.71); MD in this CT region was closest to the region of interest with regard to both chemically extracted IMF and shear-force; previous studies found MD alone to be a strong predictor of IMF (Karamichou et al., 2006; Navajas et al., 2006; Lambe et al., 2010b).

Subsequent models added CT variables in a progressive manner. Again, initially, CT variables from all reference images were used to produce prediction equations for IMF. Following on from this, information from the LV5 scan only was used and models applied in the same progressive manner.

Fifteen models were tested in the analysis independent of Pr_Cfat. Again models using reference data with more than two variables were analysed using stepwise linear regression (Genstat 14^{TM}). Models with one or two variables included were analysed using simple or multiple linear regressions, respectively.

Given the poor results obtained during the previous analyses to predict shear-force from CT information using any of the methods, or to predict IMF using virtual dissection in the LV5 image, it was decided to concentrate only on the prediction of IMF in the loin and investigate using reference information and LV5 only.

4.3.4. Single-slice and spiral x-ray CT measurements and image analysis

A series of spiral CT images were selected from the loin region of each lamb. The first image was taken where the transverse process of the 7th lumbar vertebra appears and the last image in the series where the transverse process of the 1st lumbar vertebra is no longer visible (Figure 4.3). Two-dimensional cross-sectional single-slice scans were also used, taken at two defined anatomical positions, through the top of the leg at the ischium bone (ISC), and through the chest at the 8th thoracic vertebra (TV8), details of the images used and the location are presented in Figure 4.3.

Automated analyses were performed on the images produced, to separate carcass from non-carcass tissues (Glasbey and Young, 2002), and to calculate the density of each pixel in Hounsfield units (HU).

Combining all pixels allocated as either fat or muscle enabled the use of a novel average 'soft tissue density' and its standard deviation. The spiral CT scanning (SCTS) images were used to calculate weighted average densities of muscle, fat and soft tissue (average tissue density, in each individual scan image, weighted for tissue area in that image and averaged across all images in the spiral scan series). Volumes of each tissue (mm^3) were also calculated. The resulting SCTS parameters included: weighted average muscle and fat densities and the related standard deviations; weighted average soft tissue density and standard deviation; and calculated muscle and fat volumes (mm^3). The CT variables measured from the two-dimensional single-slice scans in the ISC and TV8 regions were average muscle density, average fat density and related standard deviations, as well as the average soft tissue density and standard deviation of soft tissue density. Muscle area and fat area tissue measurements (mm^2) were also calculated for each of the single-slice scan images. Total CT predicted carcass fat (Pr_Cfat), as a measure of subcutaneous and intermuscular fat in the entire carcass, was also derived using a breed-specific prediction equation from Macfarlane et al., (2006).

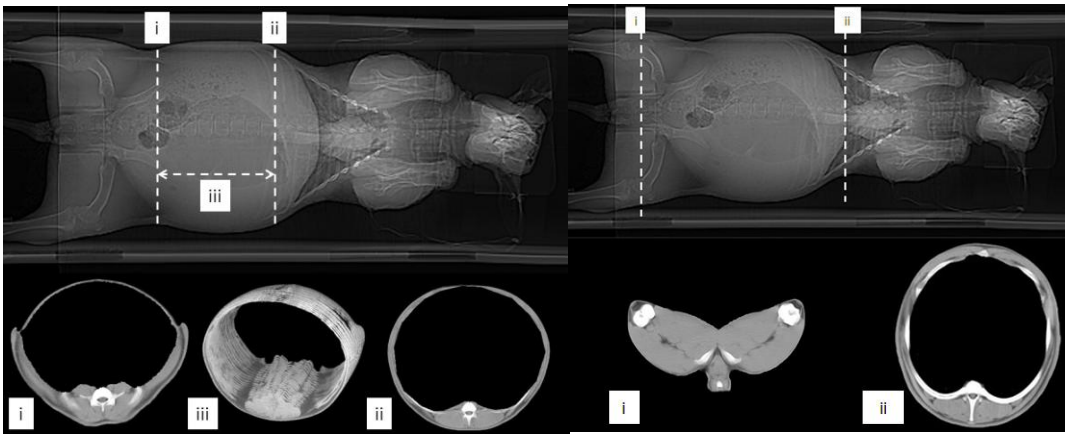

Figure 4.3 Detailed tomograms, single slice and spiral images produced during CT scanning

4.3.5. Model validation and selection

Models were then tested for significant differences using their correlation coefficient (√Adj R^2) and applying Fisher's Z transformation (Mudholkar, 2006). To make final model selections between those that predicted IMF and shear-force similarly across the whole data set, cross validation analyses were performed. Available data were split using a natural time

series separation in the data (Snee, 1977). Experiment 1 (2003-2004, n=236) data was used as the calibration data set, and Exp 2 (2009, n=134) data was used as the validation data set.

The fitted terms in the best models derived from the regression analyses of the entire data set were used to produce prediction equations using the calibration data set. These equations were then used to predict the IMF and shear-force values of animals included in the validation data. The coefficient of determination (R^2) and residual mean square error of prediction (RMSEP) were calculated for the predicted IMF percentage and shear-force (kgF) in the loin against measured values of both chemically extracted IMF and shear-force, to identify the simplest and most reliable single model or group of models.

4.4. Comparison of carcass and meat quality traits of divergent sheep genotypes and In vivo prediction of intramuscular fat content in the loins of divergent sheep genotypes using X-ray computed tomography

4.4.1. Experimental Animals

As described in section 4.1

4.4.2. Slaughter and Meat quality measurements

As described in section 4.2

4.4.3. Live animal and slaughter measurements

The data comprised of pure-bred Texel lambs (n=442) of both sexes (females and entire males), reared to weaning as singles (n=239), twins (n=176) or artificially hand-reared (n=27). The mean age at CT was 132 days (SD=19.5, ranging from 93 to 202 days), and the mean age at slaughter was 149 days (SD=21.6, ranging from 99 to 234 days). In total there were records from 442 lambs, offspring of 17 sires, and 296 dams (Table 4.3).

Table 4.3: Number of lambs for which CT was available alongside number of sires and dams within each year

Year	Lambs	Sires	Dams
2003	121	10	86
2004	115	10	80
2009	206	7	176
Total	442	17*	296*

*Sire and dam counts are not cumulative as sires and dams will have been used across years

Live weights as CT scanning and at slaughter were recorded, alongside chemical IMF levels and mechanical shear-force. Two different CT scanners were used in the combined data set utilised in this study. As different scanners were used between farms, and as we know that there is a scanner effect on density values within soft tissue ranges (Bunger et al., 2008), scanner-specific equations were developed for the scanners used (A: fixed, or B: mobile).

For the fixed scanner intramuscular fat levels in the loin were estimated from CT data using two separate prediction equations. Firstly an equation including a CT estimate of total carcass fat, and secondly using an equation independent of any CT fat weight or area measurements (PIMF1 and PIMF2 respectively, see Results section 5.2.1).

The mobile scanner equations were developed from the ones established for the fixed scanner. These were modified for the mobile scanner by fitting the optimal variables identified from the previous studies. The terms were fitted in a multiple linear regression model in Genstat14^{TM} (Payne et al., 2011), in order to produce scanner specific coefficients and assess accuracy (R^2) within the same models.

The prediction equations derived achieved accuracies of 71% and 70% for PIMF1 and PIMF2 respectively.

Scanner B: Mobile GE LightSpeed 16- slice CT scanner:

PIMF1= 5.834 + (Pr_Cfat*0.3268) - (LV5MD*0.0321) - (TV8MD*0.0915)

PIMF2 = 3.26 - (LV5MD*0.0561) - (TV8MD*0.0983) + (ISCMSD*0.1758) - (ISCFD*0.0437) - (LV5FD*0.0137) - (ISCFSD*0.0370) - (LV5FSD*0.0041)

4.4.4. Pedigree

The pedigree of the animals included in this study (8 generations) consisted of a total of 3868 records, 156 sires and 1239 dams. Lambs were the progeny of 17 sires and 296 dams over three years

4.4.5. Genetic analysis

The aim of this part of the study was to use the same experimental data set to estimate heritabilities and genetic correlations between the available traits (i.e. chemical IMF, CT estimated IMF, mechanical shear force and growth and carcass composition traits). The primary objectives of this were to estimate preliminary heritabilities of the novel CT-based predictions of IMF and laboratory based MQ measurements (chemical IMF and shear force)

and estimate genetic correlations between these CT-based predictors and post-mortem laboratory based MQ measurements (chemical IMF and shear force), which would be unavailable in any larger industry based dataset.

Genetic analyses were first attempted using an animal model. Fixed effects and covariates were analysed using ASReml 3.0 software (Gilmour et al., 2009). The model fitted to live weights at CT and slaughter included fixed effects of year born (3 levels: 2003, 2004 or 2009), age of dam at lambing (6 levels: from 2 to 7 years), sex (2 levels: entire male or female), farm (2 levels: SRUC or IBERS), rearing rank (3 levels: single, twin or artificially hand reared) and a linear covariate of age at CT scanning or age at slaughter. Analysis of meat quality traits included the same fixed effects as the previous model, but a linear covariate of live weight at slaughter, rather than age was fitted, as they were considered to be slaughter traits (Kvame and Vangen, 2007). A mixed animal model was fitted including all fixed effects and linear covariates as described above.

$$Y = Xb + Za + e$$

Y is the vector of observations on the trait of interest, *b* is a vector of the fixed effects with associated matrix *X*, *a* is the vector of additive random animal (genetic) effects with associated matrix *Z*, and *e* is the vector of random residual effect.

Only significant fixed effects and linear covariates were fitted in the final models (Table 4.4)

Following difficulties with the animal model as discussed in the results, genetic analyses were then performed using a sire model. As was previously carried out and explained for the animal model, fixed effects and covariates were analysed using ASReml 3.0 software (Gilmour et al., 2009).

A mixed sire model with pedigree was fitted including all fixed effects and linear covariates as they were described above.

$$Y = Xb + Zs + e$$

Y is the vector of observations on the trait of interest, *b* is the vector of fixed effects with associated matrix *X*. *s* is the vector of additive random sire (genetic) effects with associated matrix *Z*, and *e* is the vector of random residual effect.

Only significant fixed effects and linear covariates were fitted in the final models (Table 4.5)

Table 4.4: Significance of fixed effects and covariates for each trait analysed (Animal Model)

Trait group	Trait	Yrborn	DAMage	Sex	Farm	Rearing Rank	Cov[1]	Cov[2]	Cov[3]
Live weight	CTLWT	***	ns	***	**	***		***	
	SLWT	***	ns	***	*	***	***		
Meat Quality	ShF	***	ns	***	***	***			***
	IMF	ns	ns	***	ns	ns			***
Computed Tomography									
	CTFW	***	ns	***	ns	***		***	
	PIMF1	***	ns	***	ns	***		***	
	PIMF2	***	ns	***	ns	***		***	

Cov[1] = Age at slaughter, Cov[2] = Age at CT scanning, Cov[3] = Live weight at slaughter
*= p<0.05 ** = p<0.01, *** = p<0.001

Table 4.5: Significance of fixed effects and covariates for each trait analysed (Sire Model)

Trait group	Trait	Yrborn	DAMage	Sex	Farm	Rearing Rank	Cov[1]	Cov[2]	Cov[3]
Live weight	CTLWT	***	ns	***	***	***		***	
	SLWT	***	ns	***	*	***	***		
Meat Quality	ShF	***	ns	***	***	***			***
	IMF	ns	*	***	ns	ns			***
Computed Tomography									
	CTFW	***	ns	***	ns	***		***	
	PIMF1	***	ns	***	ns	***		***	
	PIMF2	***	ns	***	ns	***		***	

Cov[1] = Age at slaughter, Cov[2] = Age at CT scanning, Cov[3] = Live weight at slaughter
*= p<0.05, ** = p<0.01, *** = p<0.001

4.5. Genetic parameters for growth, carcass composition and intramuscular fat in Texel sheep measured by x-ray computed tomography and ultrasound

4.5.1. Animals and BASCO Database

Definitions of trait groups and variables used within the study are shown in Table 4.6

Data were extracted from the BASCO data Ltd. database, a national genetic evaluation database developed in 2004. Its purpose to store and manage very large amounts of pedigree and performance records in one single database. Originally including a co-operative of pedigree breeder associations, the Limousin cattle, and Texel and Suffolk sheep societies, pedigree and performance data is now stored on many more beef and sheep breeds.

The data set used here was restricted to Texel animals with CT scanning records and comprised records from 1971 entire male lambs from 525 sires and 1576 dams from 265 flocks over 12 years, of which 1957 animals also had records from ultrasound scanning and 1971 animals had records from CT scanning.

Full details of the number of lambs for which CT and US data were available, alongside the number of sires, dams and flocks within each year can be found in Table 4.7.

Table 4.6: Definition of variables included in the study

Trait group	Trait	Definition
Growth	8WWT	Live weight recorded at eight weeks of age
	21WWT	Live weight recorded at twenty one weeks of age (at the time of ultrasound scanning)
Ultrasound	USFD	Fat depth at the 3rd lumbar vertebra measured by ultrasound scanning (mm)
	USMD	Muscle depth at the 3rd lumbar vertebra measured by ultrasound scanning (mm)
Computed Tomography	CTFW	Carcass fat tissue weight estimated by CT (kg)
	CTMW	Carcass lean (muscle) tissue weight estimated by CT (kg)
	CTmusc	Muscularity score in the Gigot/Hind leg measured in the CT image taken at the ischium
	CTema	Area of *M. longissimus lumborum* (mm^2) measured in the CT image taken at the 5th lumbar vertebra
	PIMF1	CT predicted intramuscular fat percentage using equation 1 (%)
	PIMF2	CT predicted intramuscular fat percentage using equation 2 (%)

Table 4.7: Number of lambs for which CT and US data were available, alongside number of sires, dams and flocks within each year

Year	Lambs	Sires	Dams	Flocks
2002	87	34	76	26
2003	143	58	122	44
2004	204	70	178	61
2005	134	64	130	35
2006	89	40	82	23
2007	31	15	29	17
2008	88	33	85	21
2009	99	40	97	21
2010	166	55	155	40
2011	367	125	350	81
2012	318	97	280	71
2013	245	88	218	43
Total	1971	525*	1576*	265*

* Sires, dams and flocks are not cumulative as sires and dams will have been used across years, Flocks will record over several years

4.5.2. Growth measurements

Live weights were measured on farm at approximately eight weeks of age (mean = 66.4 days, range = 13 to 151 days) and included records from 1919 lambs, with a mean 8WWT of 31.28kg, ranging from 10.8kg to 68kg. As part of the commercial genetic evaluations in sheep, 8WWT is routinely adjusted for age, and 1867 records were available (mean = 27.26kg, range = 11.1 to 41.8kg). Live weight at twenty one week's was recorded either at twenty one weeks or at US scanning (mean = 143.3 days, range = 83 to 202 days), records were available for 1960 lambs, and mean 21WWT was 56.5kg, ranging from 26kg to 90kg.

4.5.3. Ultrasound measurements

Ultrasound data were available for lambs recorded between 2002 and 2013. Lambs were weighed and US scanned at an average age of approximately 150 days or 21 weeks. Muscle and fat depth (mm) were measured by US at the third lumbar vertebra. A single measure of muscle depth was taken, at the deepest point, and three measures of fat depth, with the first taken above the muscle at the deepest point and the following two measurements taken at 1cm lateral intervals from this point further from the backbone (Figure 4.4). All US scanning measurement, data capture and collation were carried out by Signet Breeding Services, part of EBLEX, the industry body for beef and lamb levy-payers in England.

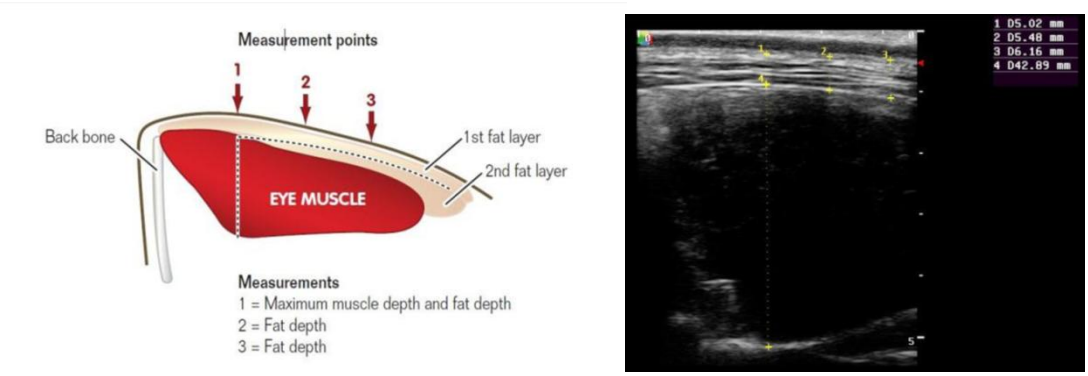

a) **b)**

Figure 4.4 (a) Diagrammatical representation of measurement points taken at ultrasound scanning (b) Ultrasound scan image of measurement points taken at scanning (Images courtesy of Sam Boon, Signet)

4.5.4. Computed tomography measurements

From 2002 to 2013 a proportion of lambs that were US scanned was then also CT scanned at the SRUC-BioSS CT unit in Edinburgh using a Siemens Somatom Esprit single slice CT scanner or at various sites across the UK using a mobile GE LightSpeed 16 slice scanner. All lambs were CT scanned within 2 weeks after US scanning. Alongside these CT measurements, routine measurement of gigot muscularity and eye muscle area (cm^2) were taken as described in Jones et al., (2002). In brief, the ratio of depth to width was taken from linear measurements on the scan image at the ischium, minus popliteal fat width, and multiplied by 100, then averaged over both legs providing a two-dimensional shape measurement in the gigot muscle (CTmusc, Figure 4.5a). Area of the *M. Longissimus lumborum* (cm^2) on both sides of the image taken at the fifth lumbar vertebra was measured and averaged to give an eye muscle area measure (CTema, Figure 4.5b). A similar muscularity measurement based on the ratio of width to depth in the *M. Longissimus lumborum* was also taken and represented in Figure 4.4b, however was not used in this study.

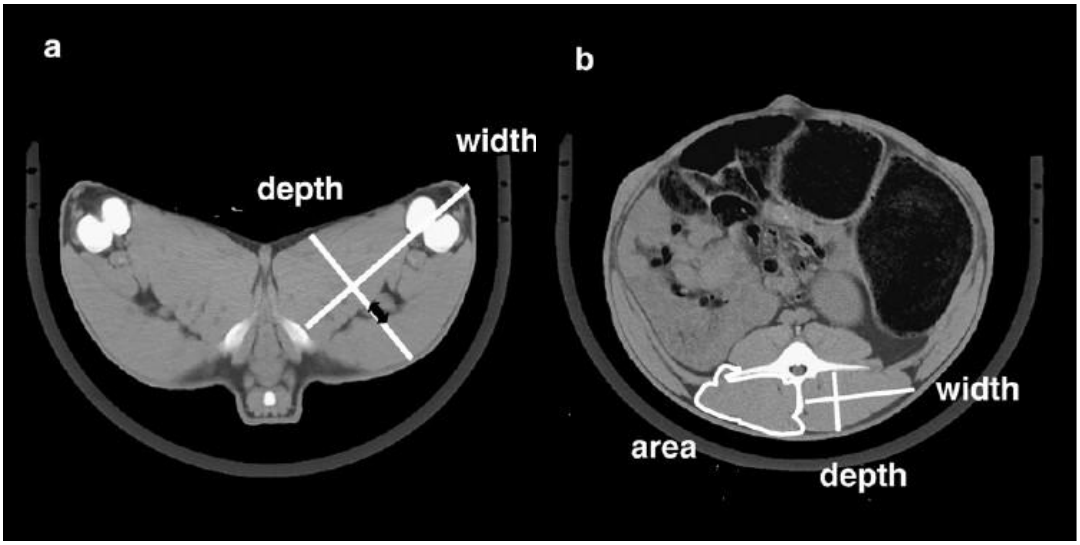

Figure 4.5a Measurements taken on the scan image taken at the ischium to calculate CTmusc (a) and measurements taken on the image taken at the fifth lumbar vertebra to calculate CTema (b)

4.5.5. CT predictions of intramuscular fat

Intramuscular fat content in the loin was predicted using two separate prediction equations, firstly an equation including a CT prediction of total carcass fat weight (PIMF1) and, secondly, using a prediction equation entirely independent of any CT fat area or weight measurements (PIMF2).

As different scanners were employed through the period of data collection from 2002-2013, and as we know that there is a scanner effect on density values within soft tissues (Bunger et al., 2008), scanner-specific equations were developed for scanner type used (A: fixed, or B: mobile) as described in section 4.5.1.

5. Results

5.1. In vivo prediction of intramuscular fat content and shear-force in Texel lamb loins using x-ray computed tomography

Table 5.1: Linear regression models between IMF, shear force and CT tissue density parameters including Pr_Cfat, with adjusted coefficient of determination (Adj R2) and residual mean square error (RMSE), based on the whole data set (n=370)

		Shear force (Log10)				IMF			
		Ref[1]		LV5[2]		Ref[1]		LV5[2]	
	Maximum Model	**Adj R^2**	**RMSE**	**Adj R^2**	**RMSE**	**Adj R^2**	**RMSE**	**Adj R^2**	**RMSE**
A	Pr_Cfat	0.03	0.16	0.03	0.16	0.51	0.48	0.51	0.48
B	Pr_Cfat+MD	0.07	0.16	0.05	0.16	0.66[ab]	0.40	0.63[ab]	0.41
C	Pr_Cfat+FD	0.05	0.16	0.04	0.16	0.54	0.47	0.54	0.47
D	Pr_Cfat+MA	0.04	0.16	0.03	0.16	0.60[b]	0.43	0.56	0.45
E	Pr_Cfat+FA	0.10[a]	0.16	0.04	0.16	0.57	0.45	0.53	0.47
F	Pr_Cfat+MD+FD	0.07	0.16	0.05	0.16	0.67[ab]	0.40	0.63[ab]	0.41
G	Pr_Cfat+MA+FA	0.11[a]	0.16	0.05	0.16	0.60[b]	0.43	0.56	0.45
H	Pr_Cfat+MD+MSD	0.09	0.16	0.07	0.16	0.66[ab]	0.40	0.64[ab]	0.41
I	Pr_Cfat+FD+FSD	0.10[a]	0.16	0.07	0.16	0.56	0.46	0.55	0.46
J	Pr_Cfat+MD+MSD+FD+FSD	0.12[a]	0.16	0.09	0.16	0.67[ab]	0.39	0.64[ab]	0.41
K	Pr_Cfat+MD+MSD+FD+FSD+FA	0.14[a]	0.15	0.09	0.16	0.67[ab]	0.39	0.65[ab]	0.41
L	Pr_Cfat+MD+MSD+FD+FSD+MA+FA	0.14[a]	0.15	0.09	0.16	0.68[ab]	0.39	0.66[ab]	0.40
M	Pr_Cfat+STD	0.08	0.16	0.05	0.16	0.64[ab]	0.41	0.60[b]	0.43
N	Pr_Cfat+STD+STSD	0.09	0.16	0.05	0.16	0.68[ab]	0.39	0.64[ab]	0.41
O	Pr_Cfat+STD+STSD+FA	0.10[a]	0.16	0.05	0.16	0.68[ab]	0.39	0.64[ab]	0.41
P	Pr_Cfat+STD+STSD+FA+MA	0.11[a]	0.16	0.05	0.16	0.68[ab]	0.39	0.65[ab]	0.40

Ref[1]; using information from all three reference scans, LV5[2]; using information from LV5 scan only

[a] Adj R^2 values are significantly greater than model A ($P<0.05$)

[b] Adj R^2 values do not differ significantly from model L^{ref} (IMF benchmark)

5.1.1. Models inclusive of CT estimated carcass fat

Mean IMF was 1.48% (SD = 0.68) and ranged from 0.27 to 3.88%. Mean shear force was 3.4kgF (SD = 1.56, ranging from 1.39-10.72kgF). Pr_Cfat alone accounted for no variation in shear force (Adj R^2 = 0.03). Following stepwise linear regression analysis the accuracy was significantly increased ($P<0.05$, Adj R^2 = 0.10) by also including fat area measured in the ischium (ISCFA) and 8th thoracic vertebra (TV8FA) scans. The accuracy was further improved, but not significantly, to a maximum Adj R^2 = 0.14, with the inclusion of standard deviation of fat density in the ischium and 5th lumbar vertebra scans (ISCFSD, LV5FSD), standard deviation of muscle density in the ischium and 8th thoracic vertebra scans

(ISCMSD, TV8MSD), muscle density in the ischium scan (ISCMD) and fat area in the ischium, fifth lumbar vertebra and 8th thoracic vertebra scans (ISCFA, LV5FA, TV8FA). As expected, Pr_Cfat alone accounted for a moderate amount of the variation in IMF (Adj R^2 = 0.51).

For IMF, ten models out of the fifteen models tested (not including the 'baseline') included additional CT variables, with statistically significant improvement in accuracy of prediction when compared to Pr_Cfat as a single predictor (P<0.05). Models C^{ref}, D^{ref}, E^{ref}, G^{ref} and I^{ref} were shown not to be significantly different in prediction accuracy from Pr_Cfat (A^{ref}) (Adj R^2 = 0.54, 0.60, 0.57, 0.60 and 0.56 respectively). All other models were >Adj R^2 = 0.63 (Table 5.1).

From these ten models, the model with the highest Adj R^2 value was identified (Model L^{ref}; Adj R^2 = 0.68), which included areas, average densities and density standard deviations for both fat and muscle in the maximum model. The fitted terms included average muscle density from the LV5 and TV8 scans. This model was then used as a benchmark model in order to compare the ten models identified as better predictors of IMF from reference scan information than Pr_Cfat alone.

Models with statistically significantly lower accuracy (P<0.05) compared to the benchmark model (L^{ref}) were discarded. All ten original models identified were retained, however the final fitted terms in models B^{ref} and H^{ref} were identical following the stepwise procedure, and as a result model H^{ref} was discarded. This left nine models (including the benchmark model L^{ref}) with correlation coefficients that were not significantly different from one another, meaning that the prediction ability of these nine models is statistically similar. Therefore, a group of models was identified that would equally well predict IMF using different combinations of reference scan information. These models included M^{ref} (Adj R^2 0.64), B^{ref} (Adj R^2 0.66), F^{ref}, J^{ref}, K^{ref} (Adj R^2 0.67), L^{ref}, N^{ref}, O^{ref}, P^{ref} (Adj R^2 0.68).

The use of information from the LV5 scan image only to predict shear force was poor, producing a maximum accuracy of Adj R^2 = 0.09 (Table 5.1). Given these low accuracies in the prediction of shear force, further cross validation and progressive image analysis was only carried out in the prediction of IMF. Models using only information from the LV5 scan image to predict IMF were again compared to the simple linear model using only Pr_Cfat and nine models were identified as being significantly more accurate in the prediction of IMF. These models were B^{LV5}, F^{LV5} (Adj R^2 0.63), H^{LV5}, J^{LV5}, N^{LV5}, O^{LV5} (Adj R^2 0.64), K^{LV5}, P^{LV5} (R^2 0.65) and L^{LV5} (Adj R^2 0.66).

Model B^{LV5} and F^{LV5} resulted in the same final fitted terms following the stepwise procedure, so F^{LV5} was discarded, leaving eight final models shown not to be significantly different ($P<0.05$) from the benchmark model (L^{ref}). These eight models were then tested for significance against the model including the largest amount of explanatory variables from the group of models identified as most accurate in explaining the variation of IMF (Model L^{ref}) in the entire data set. All eight models were retained, as none were shown to be significantly different from model L^{ref} ($P<0.05$).

Image analysis then considered the use of regions of interest (ROI) taken from the LV5 scan, comparing the use of information from: (i) the full LV5 scan (LV5); (ii) Dissect[1]; or (iii) Dissect[2] (Figure 4.2). Models were again compared using the correlation coefficient of each model and tested for significant differences using Fisher's Z transformation.
There was no significant improvement in accuracy at any stage during the virtual dissection of the LV5 image, and in many cases there was a decrease in accuracy, compared to using data from the full LV5 image, although again not a significant decrease (Table 5.2). Furthermore, there was no significant improvement in the accuracy of the models within ROI method from employing additional information from CT variables.

Table 5.2: Linear regression models between IMF and CT tissue density parameters during virtual dissection, with adjusted coefficient of determination (R2) and residual mean square error (RMSE), based on the subset of the data (n=100)

		LV5		Dissect[1]		Dissect[2]	
	Model	**Adj R^2**	**RMSE**	**Adj R^2**	**RMSE**	**Adj R^2**	**RMSE**
A	Pr_Cfat	0.43	0.54	0.43	0.54	0.43	0.54
B	Pr_Cfat+MD	0.61	0.45	0.54	0.49	0.55	0.48
C	Pr_Cfat+FD	0.47	0.52	0.43	0.54	0.44	0.54
D	Pr_Cfat+MA	0.48	0.52	0.49	0.51	0.49	0.51
E	Pr_Cfat+FA	0.44	0.54	0.43	0.54	0.43	0.54
F	Pr_Cfat+MD+FD	0.61	0.45	0.54	0.49	0.58	0.47
G	Pr_Cfat+MA+FA	0.48	0.52	0.49	0.51	0.49	0.51
H	Pr_Cfat+MD+MSD	0.61	0.45	0.54	0.49	0.55	0.48
I	Pr_Cfat+FD+FSD	0.48	0.52	0.45	0.53	0.46	0.53
J	Pr_Cfat+MD+MSD+FD+FSD	0.61	0.44	0.55	0.48	0.59	0.46
K	Pr_Cfat+MD+MSD+FD+FSD+FA	0.61	0.44	0.55	0.48	0.59	0.46
L	Pr_Cfat+MD+MSD+FD+FSD+MA+FA	0.62	0.44	0.57	0.47	0.62	0.44
M	Pr_Cfat+STD	0.54	0.49	0.52	0.50	0.53	0.49
N	Pr_Cfat+STD+STSD	0.56	0.47	0.54	0.48	0.55	0.48
O	Pr_Cfat+STD+STSD+FA	0.60	0.45	0.55	0.48	0.55	0.48
P	Pr_Cfat+STD+STSD+FA+MA	0.61	0.45	0.58	0.47	0.58	0.47

LV5; Using information from LV5 only, Dissect[1]; using information from dissect1 CT variables, Dissect [2]; using information from dissect2 CT variables

5.1.2. Model validation and selection

These analyses identified seventeen models that were shown to be statistically similar in their prediction accuracies of IMF, including either information from the reference scans or LV5 scan only.

The final seventeen models identified were then used to perform cross validation analysis. Seventeen prediction equations were derived using the validation data set, corresponding to the seventeen 'best' models identified from primary analysis (Table 5.3). The models were then used to predict the IMF values of animals included in the validation data. Coefficients of determination (R^2) and error of prediction (RMSEP) for the predicted IMF percentage in the loin against chemically extracted IMF are also shown in Table 5.3.

The models with the strongest cross validity were models M^{ref} (R^2_{cal} 0.64, R^2_{val} 0.67) and N^{ref} (R^2_{cal} 0.67, R^2_{val} 0.67), using soft tissue density information from all three reference scans (M^{ref}) and using soft tissue density information from the LV5 and TV8 scans alongside the standard deviation of soft tissue density from all three reference scans (N^{ref}). Residual mean square error of prediction (RMSEP) in the validation data compared to the calibration data, decreased slightly across all models. The reduction of RMSEP is due to the characteristics of the validation data set. The reduction in variation of IMF across the validation data set reduces the error of the prediction. These models were then used as a benchmark and all other models were tested for significant differences in correlation coefficients using Fisher's Z transformation (Mudholkar, 2006). All seventeen models were found to be statistically similar in prediction accuracy ($P<0.05$) and no significant reduction in prediction accuracy was seen across the calibration and validation models.

From this, two models were chosen from the criteria of firstly, the simplest and best models (N^{ref}) and the simplest model that was shown to be significantly more accurate in prediction than the baseline (B^{ref}). Final models are shown below.

A: Pr_IMF_Bref (Pr_IMF_A) (%) = 6.920 + (Pr_Cfat*0.2425) - (LV5MD*0.0654) – (TV8MD*0.0637)

B: Pr_IMF_Nref (Pr_IMF_B) (%) = 7.320 + (Pr_Cfat*0.0565) – (LV5STD*0.0626) – (TV8STD*0.03585) + (ISCSTSD*0.02209) – (LV5STSD*0.0565) – (TV8STSD*0.0303)

Table 5.3: Linear regression models between IMF and CT tissue density parameters including Pr_Cfat, with adjusted coefficient of determination (R2) and residual mean square error (RMSE), based on the training data set (n=236) and validation data set (n=134

		Calibration (n=236)		Validation (n=134)	
	Fitted Terms	**Adj R^2**	**RMSE**	**Adj R^2**	**RMSEP**
B^{ref}	Pr_Cfat, LV5MD, TV8MD	0.69	0.41	0.63	0.33
F^{ref}	Pr_Cfat, LV5MD, TV8MD, ISCFD	0.69	0.41	0.63	0.33
J^{ref}	Pr_Cfat, LV5MD, TV8MD, ISCFD, LV5FSD	0.69	0.41	0.64	0.32
K^{ref}	Pr_Cfat, LV5MD, TV8MD, ISCFA, LV5FA	0.70	0.41	0.63	0.32
L^{ref}	Pr_Cfat, LV5MD, TV8MD, LV5FD, ISCMA, LV5FA, TV8FA	0.71	0.41	0.65	0.32
M^{ref}	Pr_Cfat, ISCSTD, LV5STD, TV8STD	0.64	0.45	0.67	0.31
N^{ref}	Pr_Cfat, LV5STD, TV8STD, ISCSTSD, LV5STSD, TV8STSD	0.67	0.42	0.67	0.30
O^{ref}	Pr_Cfat, ISCSTD, ISCSTSD, LV5STD, LV5STSD, TV8STD, ISCFA, TV8FA, ISCFA	0.68	0.42	0.66	0.31
P^{ref}	Pr_Cfat, LV5STD, LV5STSD, TV8STD, TV8STSD, ISCMA, TV8FA	0.69	0.41	0.66	0.31
B^{LV5}	Pr_Cfat, LV5MD	0.67	0.43	0.57	0.35
H^{LV5}	Pr_Cfat, LV5MD, LV5MSD	0.67	0.43	0.59	0.35
J^{LV5}	Pr_Cfat, LV5MD, LV5FD, LV5FSD	0.68	0.42	0.57	0.35
K^{LV5}	Pr_Cfat, LV5MD, LV5FSD, LV5FA	0.68	0.42	0.59	0.35
L^{LV5}	Pr_Cfat, LV5MD, LV5FD, LV5MA, LV5FA	0.68	0.42	0.60	0.34
N^{LV5}	Pr_Cfat, LV5STD, LV5STSD	0.64	0.44	0.61	0.34
O^{LV5}	Pr_Cfat, LV5STD, LV5STSD, LV5FA	0.64	0.44	0.61	0.34
P^{LV5}	Pr_Cfat, LV5STD, LV5STSD, LV5MA	0.66	0.43	0.62	0.33

5.1.3. Models independent of CT estimated carcass fat

Given the poor results obtained during the previous analyses to predict shear force from CT information using any of the methods, or to predict IMF using virtual dissection in the LV5 image, it was decided to concentrate only on the prediction of IMF in the loin and investigate using reference information and LV5 only.

As expected, MD in the reference scans accounted for a moderate amount of variation in IMF (Adj R^2 = 0.60). There was no model, from the 14 models tested not including the baseline model (MD), with statistically significant improvement in prediction accuracy, however five models were significantly lower in in accuracy of prediction when compared to the baseline model ($P<0.05$). Models B^{ref_ex}, C^{ref_ex}, D^{ref_ex}, F^{ref_ex} and H^{ref_ex} were therefore dropped from further analysis.

From the remaining ten models, the model with the highest Adj R^2 value was chosen as a benchmark model (Model K^{ref_ex}; Adj R^2 = 0.68), all remaining models were tested for significant differences in prediction accuracy to the benchmark (K^{ref_ex}). All ten models were shown to have no significant difference in accuracy ($P<0.05$), however, following the stepwise procedure during the regression analysis, final parameters fitted to model M^{ref_ex}, N^{ref_ex} and O^{ref_ex} were identical and as a result models N^{ref_ex} and O^{ref_ex} were discarded.

The remaining eight models included A^{ref_ex} (Adj R^2 = 0.60), E^{ref_ex}, L^{ref_ex} (Adj R^2 = 0.63), G^{ref_ex} (Adj R^2 = 0.61), I^{ref_ex} (Adj R^2 = 0.66), K^{ref_ex} (Adj R^2 = 0.68) and M^{ref_ex} (Adj R^2 = 0.67) all not significantly different in their prediction ability (Table 5.4).

Models using the CT parameter information from the LV5 scan only were again compared to the baseline model including only LV5MD. A moderate amount of the variation in IMF could be explained by the use of LV5MD alone (Adj R^2 = 0.51). Six models were found to be significantly more accurate in the prediction IMF. These models were M^{LV5_ex} (Adj R^2 = 0.61), I^{LV5_ex}, N^{LV5_ex}, O^{LV5_ex} (Adj R^2 = 0.62), J^{LV5_ex} and K^{LV5_ex} (Adj R^2 = 0.64).

Model N^{LV5_ex} and O^{LV5_ex} included the same CT variables in the final fitted models following the stepwise procedure, therefore model O^{LV5_ex} was discarded. Models were then subsequently tested for significant differences against the benchmark model (K^{LV5_ex}), chosen on Adj R^2 value and number of parameters included in the model as previously explained. All models were retained, as none were shown to be significantly different from model K^{LV5_ex} ($P<0.05$) (Table 5.4). Model L^{LV5_ex} was not significantly greater in prediction accuracy than the baseline (A^{LV5_ex}), however it was also not significantly different in

accuracy from the benchmark model (K^{LV5_ex}) (Table 5.4). As a result of this, and because there were a number of models available, model L^{LV5_ex} was discarded.

Table 5.4: Linear regression models between IMF CT tissue density parameters in models excluding Pr_Cfat, with adjusted coefficient of determination (Adj R2) and residual mean square error (RMSE), based on the whole data set (n=370)

		IMF			
		Ref[1]		LV5[2]	
	Maximum Model	**Adj R^2**	**RMSE**	**Adj R^2**	**RMSE**
A	MD	0.60[b]	0.44	0.51	0.48
B	FD	0.40	0.53	0.22	0.60
C	MA	0.07	0.66	0.07	0.66
D	FA	0.57	0.45	0.51	0.48
E	FD	0.63[b]	0.42	0.22	0.60
F	MA+FA	0.58	0.44	0.51	0.48
G	MD+MSD	0.61[b]	0.43	0.55	0.46
H	FD+FSD	0.53	0.47	0.50	0.48
I	MD+MSD+FD+FSD	0.66[b]	0.40	0.62[ab]	0.42
J	MD+MSD+FD+FSD+FA	0.67[b]	0.39	0.64[ab]	0.41
K	MD+MSD+FD+FSD+FA+MA	0.68[b]	0.39	0.64[ab]	0.41
L	STD	0.63[b]	0.42	0.58[b]	0.45
M	STD+STSD	0.67[b]	0.39	0.61[ab]	0.43
N	STD+STSD+FA	0.67[b]	0.39	0.62[ab]	0.42
O	STD+STSD+FA+MA	0.67[b]	0.39	0.62[ab]	0.42

Ref[1]; using information from all three reference scans, LV5[2]; using information from LV5 scan only
[a] Adj R^2 values are significantly greater than model A ($P<0.05$)
[b] Adj R^2 values do not differ significantly from model K^{ref} (IMF benchmark)

5.1.4. Model validation and selection

The analysis of models using both entire reference scan information and LV5 scan only information identified thirteen potential models in the prediction of IMF. All thirteen models were statistically similar in accuracy. These final thirteen models were then cross validated using the same time series data split, and the same calibration and validation data sets as described above. Thirteen prediction equations were derived using the calibration data set (Table 5.5). The models were again used to predict the IMF values of animal included in the validation data. Coefficients of determination (R^2) and error of prediction (RMSEP) are shown in Table 5.5. The model with the strongest cross validity was model M^{ref_ex} (R^2_{cal} 0.68, R^2_{val} 0.67), using soft tissue density information from all three reference scans. However, no model's validation accuracy fell significantly when compared to calibration accuracies ($P<0.05$).

It was also recognised that not all models were entirely independent of the amount of CT measured carcass fat in the lamb, as, although Pr_Cfat was not included in the models, some models in the analysis included CT-measured fat areas (FA) so were not independent

of overall amount of carcass fat. Therefore, models J^{ref_ex}, K^{ref_ex}, J^{LV5_ex}, K^{LV5_ex} and N^{LV5_ex} were not considered for selection. From the remaining models, one model was selected on the basis of the single best model employing CT parameter information which is routinely collected during current practices at SRUC (I^{ref_ex}) using information from the reference scans, including MD, MSD, FD and FSD. The final selected model is shown below (Adj R^2 = 0.67 with the full data set):

Pr_IMF_Iref_ex (%) = 7.26-(0.0720*LV5MD) - (0.0611*TV8MD) + (0.0748*ISCMSD) - (0.02090*ISCFD) - (0.00758*LV5FD) - (0.0344*ISCFSD) - (0.0324*LV5FSD)

Table 5.5: Linear regression models between IMF and CT tissue density parameters excluding Pr_Cfat, with adjusted coefficient of determination (R2) and residual mean square error (RMSE), based on the training data set (n=236) and validation data set (n=134)

		Calibration (n=236)		**Validation (n=134)**	
	Fitted Terms	**Adj R^2**	**RMSE**	**Adj R^2**	**RMSE**
A^{ref_ex}	ISCMD, LV5MD, TV8MD	0.65	0.44	0.56	0.36
E^{ref_ex}	ISCMD, LV5MD, TV8MD, ISCFD, LV5FD, TV8FD	0.67	0.42	0.59	0.34
G^{ref_ex}	ISCMD, LV5MD, TV8MD, ISCMSD, LV5MSD	0.67	0.42	0.63	0.33
I^{ref_ex}	LV5MD, TV8MD, ISCMSD, ISCFD, LV5FD, ISCFSD, LV5FSD	0.70	0.41	0.63	0.33
J^{ref_ex}	LV5MD, TV8MD, LV5FD, ISCFA, LV5FA	0.70	0.41	0.64	0.32
K^{ref_ex}	LV5MD, TV8MD, LV5FD, ISCFA, LV5FA, ISCMA, TV8MA	0.70	0.40	0.65	0.32
L^{ref_ex}	ISCSTD, LV5STD, TV8STD	0.64	0.45	0.66	0.31
M^{ref_ex}	LV5STD, TV8STD, ISCSTSD, LV5STSD, TV8STSD	0.68	0.42	0.67	0.31
I^{LV5_ex}	LV5MD, LV5MSD, LV5FD, LV5FSD	0.67	0.42	0.57	0.35
J^{LV5_ex}	LV5MD, LV5FD, LV5FA	0.67	0.42	0.57	0.35
K^{LV5_ex}	LV5MD, LV5FD, LV5FA, LV5MA	0.68	0.42	0.58	0.35
M^{LV5_ex}	LV5STD, LV5STSD	0.63	0.45	0.59	0.34
N^{LV5_ex}	LV5STD, LV5STSD, LV5FA	0.63	0.45	0.59	0.34

5.2. Prediction of intramuscular fat content and shear-force in Texel lamb loins using combinations of different in vivo x-ray computed tomography (CT) scanning techniques

Table 5.6: Regression results for the prediction of shear force and IMF, presented are the adjusted coefficient of determination (Adj R2) and residual mean square error (RMSE) using information from SCTS only (sp) or a combination of SCTS and two dimensional single-slice scans (com)

	Shear Force				**IMF**			
	sp		**com**		**sp**		**com**	
Model	**Adj R^2**	**RMSE**	**Adj R^2**	**RMSE**	**Adj R^2**	**RMSE**	**Adj R^2**	**RMSE**
A	0.03	0.16	0.03	0.16	0.50	0.47	0.50	0.47
B	0.03	0.16	0.07	0.16	0.67**	0.39	0.68**	0.39
C	0.04	0.16	0.05	0.16	0.51	0.48	0.52	0.48
D	0.04	0.16	0.04	0.16	0.56	0.46	0.60	0.43
E	0.03	0.16	0.10*	0.16	0.55	0.46	0.58	0.45
F	0.04	0.16	0.09	0.16	0.68**	0.39	0.70**	0.38
G	0.04	0.16	0.10*	0.16	0.58	0.45	0.60	0.43
H	0.04	0.16	0.09	0.16	0.67**	0.39	0.68**	0.39
I	0.05	0.16	0.09	0.16	0.55	0.46	0.56	0.46
J	0.05	0.16	0.12*	0.16	0.69**	0.38	0.70**	0.37
K	0.05	0.16	0.13*	0.15	0.69**	0.38	0.70**	0.37
L	0.06	0.16	0.13*	0.15	0.70**	0.38	0.71**	0.37
M	0.02	0.16	0.08	0.16	0.54	0.47	0.63*	0.42
N	0.02	0.16	0.09	0.16	0.57	0.45	0.66**	0.40
O	0.03	0.16	0.10*	0.16	0.59	0.44	0.67**	0.40
P	0.04	0.16	0.10*	0.16	0.62*	0.42	0.67**	0.39

sp Using SCTS information
com Using a combination of SCTS and single-slice CT information
*Adj R^2 differs significantly from the baseline model (A) (P > 0.05)
**Adj R^2 does not differ significantly from the most accurate model (L) (P < 0.05)

5.2.1. Predicting shear force and IMF content using SCTS information

Very little of the variation in shear force was accounted for by Pr_Cfat (Adj R^2 = 0.03, RMSE = 0.16), however Pr_Cfat accounted for a moderate amount of the variation in IMF (Adj R^2 = 0.50, RMSE = 0.47). Compared to the baseline, which uses information only from CT derived predicted carcass fat, seven models that included additional spiral CT variables, from the fifteen models tested, were identified as being significantly more accurate in the prediction of IMF (P < 0.05). None of the models using only spiral CT information (^{sp}) were significantly more accurate (P > 0.05) in prediction of shear force when compared to the baseline (Table 5.6).

From the seven models using only SCTS information identified with significantly increased prediction ability of IMF when compared to Model A, the model with the greatest accuracy was identified as model L^{sp} (Adj R^2 = 0.70). This model included CT predicted carcass fat (Pr_Cfat), weighted average muscle density (w_md), fat volume and muscle volume (f_vol, m_vol), resulting in the prediction equation:

$$y = 7.773 + 0.1808 \times PrCfat - 0.1379 \times w\_md + 0.000000881 \times f\_vol - 0.0000000338 \times m\_vol.$$

The six remaining models including only SCTS information identified as better predictors of IMF than Pr_Cfat alone were compared with model L^{sp}. Only model P^{sp} (Table 5.6) gave significantly reduced accuracy (P > 0.05) compared to model L^{sp}. This left six models with correlation coefficients that were not significantly different, essentially meaning that the prediction ability of these six models is statistically similar, thus identifying a group of models that would predict IMF equally using SCTS information. The variables for models K^{sp} and J^{sp} after the stepwise regression procedure were identical and, hence, model K^{sp} was also dropped. The final selected models were model B^{sp} (Adj R^2 = 0.67), model F^{sp} (Adj R^2 = 0.68), model H^{sp} (Adj R^2 = 0.67), model J^{sp} (Adj R^2 = 0.69) and model L^{sp} (Adj R^2 = 0.70).

5.2.2. Predicting shear-force and IMF content using a combination of SCTS and single-slice scan information

Models using a combination of SCTS information and single-slice scan information (^{com}) were compared to the simple linear model using only Pr_Cfat for the predictions of both shear force and IMF. In the analysis for the prediction of shear force, prediction accuracies were significantly improved with the inclusion of information from the single-slice scan images (ISC, TV8). Nonetheless, the overall results show that the maximum prediction accuracy achieved for shear force, from models developed was Adj R^2 = 0.13 (Table 5.6).

In the prediction of IMF, ten of the fifteen models tested were significantly greater in prediction accuracies than that of Pr_Cfat alone (P < 0.05). From these models the single 'best' model was identified as model L^{com} (Adj R^2 = 0.71):

$$y = 7.675 + 0.3125 * PrCfat - 0.0978 \times w\_md + 0.0000000299 \times m\_vol + 0.000001196 \times f\_vol + 0.0168 \times ISCMD + 0.0371 \times ISCMSD - 0.0000393 \times ISCMA - 0.0543 \times TV8MD + 0.0000236 \times TV8MA - 0.0001298 \times TV8FA.$$

All models identified as significant previously were then tested against model L^{com} and any that were significantly different in prediction accuracy were discarded (P > 0.05), the only model identified was model M^{com} (Adj R^2 = 0.63). These analyses therefore identified nine "best" models with similar prediction abilities: L^{com} (Adj R^2 = 0.71); F^{com}, J^{com} and K^{com} (Adj R^2

= 0.70); B^{com} and H^{com} (Adj R^2 = 0.68); O^{com} and P^{com} (Adj R^2 = 0.67); and N^{com} (Adj R^2 = 0.66). Regression results for all models are presented in Table 5.6.

5.2.3. Model cross-validation and selection

Table 5.7: Cross-validation results: adjusted coefficient of determination (Adj R2), residual mean square error (RMSE) of calibration; and coefficient of determination (R2) and residual mean square error of prediction (RMSEP) of the validation data

Model	**Calibration (n=236)**		**Validation (n=134)**	
	Adj R^2	**RMSE**	**R^2**	**RMSEP**
B^{sp}	0.69	0.41	0.60	0.34
F^{sp}	0.70	0.41	0.59	0.34
H^{sp}	0.69	0.41	0.60	0.34
J^{sp}	0.70	0.41	0.62	0.33
L^{sp}	0.71	0.40	0.62	0.33
B^{com}	0.71	0.40	0.64	0.32
F^{com}	0.71	0.40	0.64	0.32
H^{com}	0.70	0.40	0.64	0.32
J^{com}	0.72	0.40	0.66	0.31
K^{com}	0.71	0.40	0.65	0.32
L^{com}	0.72	0.39	0.65	0.32
N^{com}	0.66	0.43	0.67	0.31
O^{com}	0.67	0.43	0.64	0.32
P^{com}	0.67	0.42	0.64	0.32

^{sp} Model uses information from spiral scans only
^{com} Model uses information from a combination of spiral and two dimensional scans

Table 5.8: Final prediction models and equations derived from the whole data set, adjusted coefficient of determination (Adj R2) and residual mean square error of the prediction (RMSEP)

Model	Final prediction model equation	Adj R^2	RMSEP
B^{sp}	y=8.048+0.2508*Pr_Cfat-0.1551*w_md	0.67	0.39
F^{sp}	y=7.897+0.2347*Pr_Cfat-0.1720*w_md-0.01514*w_fd	0.68	0.39
H^{sp}	y=7.10+0.2326*Pr_Cfat-0.1474*w_md+0.0319*w_msd	0.67	0.39
J^{sp}	y=7.62+0.1134*Pr_Cfat-0.1566*w_md+0.0401*w_mSD-0.02682*w_fd-0.0417*w_fsd	0.69	0.38
L^{sp}	y=7.773+0.1808*Pr_Cfat-0.1379*w_md+0.000000881*f_vol-0.000000038*m_vol	0.70	0.38
B^{com}	y=8.275+0.2248*Pr_Cfat-0.1113*w_md-0.0490*TV8MD	0.68	0.39
F^{com}	y=7.794+0.1704*Pr_Cfat-0.1347*w_md-0.01553*w_fd+0.0183*ISCMD-0.0600*TV8MD-0.00471*TV8FD	0.70	0.38
H^{com}	y=7.39+0.2079*Pr_Cfat-0.1043*w_md+0.0298*w_mSD-0.0488*TV8MD	0.68	0.39
J^{com}	y=6.66+0.1054*Pr_Cfat-0.1138*w_md+0.0661*w_mSD-0.02761*w_fd-0.0250*w_fSD-0.0502*TV8MD	0.70	0.37
K^{com}	y=5.78-0.1051*w_md+0.0549*w_mSD-0.01753*w_fd+0.000000769*f_vol+0.0437*ISCMSD-0.00703*ISCFD-0.0189*ISCFSD-0.0533*TV8MD	0.70	0.37
L^{com}	y=7.675+0.3125*Pr_Cfat-0.0978*w_md-0.000000299*m_vol+0.000001196*f_vol+0.0168*ISCMD+0.0371*ISCMSD-0.0000393*ISCMA-0.0543*TV8MD+0.0000236*TV8MA-0.0001298*TV8FA	0.71	0.37
N^{com}	y=7.099+0.1101*Pr_Cfat-0.0305*w_std-0.0368*w_stSD-0.0205*ISCSTD-0.04523*TV8STD+0.0103*ISCSTSD-0.0404*TV8STSD	0.66	0.40
O^{com}	y=7.382+0.2253*Pr_Cfat-0.0251*w_std-0.0332*w_stSD+0.000001035*f_vol-0.0322*ISCSTD+0.0142*ISCSTSD-0.04967*TV8STD-0.0387*TV8STSD-0.0001178*ISCFA-0.0001394*TV8FA	0.67	0.40
P^{com}	y=8.554+0.4879*Pr_Cfat-0.0330*w_std-0.0448*w_stSD+0.000001051*f_vol-0.000000243*m_vol-0.0000566*ISCMA-0.05713*TV8STD-0.0357*TV8STSD-0.0002859*TV8FA+0.0000371*TV8MA	0.67	0.39

^{sp} Model uses information from Pr_Cfat and spiral scans only

^{com} Model uses information from Pr_Cfat and a combination of spiral and single-slice scans

Given the poor prediction abilities of CT for shear force using the parameters tested, cross-validation analysis for the prediction of shear force was not carried out. Fourteen possible models in the prediction of IMF were identified. None of these models had significantly less prediction accuracy (P > 0.05) than the single 'best' model from both SCTS information and a combination of SCTS information and single-slice scan information (Model L^{com}), so all were retained for cross-validation analyses. For cross-validation, fourteen prediction equations were derived using the calibration data set (n = 236), corresponding to the independent variables identified in the final selected models from the original stepwise regression analyses. The models were then used to predict the chemical IMF values of lambs in the independent validation data set (n = 134). Final cross-validation results,

coefficients of determination (R^2) and residual mean square errors of prediction (RMSEP) are presented in Table 5.7.

The model with the strongest cross-validity was model N^{com} (R^2 = 0.67, RMSEP = 0.40) using both SCTS information and single-slice scan information, including CT predicted carcass fat (Pr_Cfat), weighted average density of soft tissue and its standard deviation (w_std and w_stsd) in the spiral scan of the loin, average soft tissue density and its standard deviation in the ischium scan (ISCSTD and ISCSTSD), average soft tissue density in the 8th thoracic vertebra scan and its standard deviation (TV8STD and TV8STSD). The R^2 of this model (N^{com}, R^2 = 0.67) was compared with the thirteen remaining models in the cross-validation analysis using Fisher's z transformation (Mudholkar, 2006). All of the models performed as well as model N in the cross-validation analysis ($P < 0.05$; R^2 = 0.59 to 0.66). This left fourteen models for consideration as predictors of IMF, five of which used only SCTS information alongside Pr_Cfat, and nine of which used a combination of SCTS information and single-slice information alongside Pr_Cfat. Details of the final selected prediction models developed from the entire data set are presented in Table 5.8. These included Models B^{sp}, F^{sp}, H^{sp}, J^{sp} and L^{sp} using SCTS information and models B^{com}, F^{com}, H^{com}, J^{com}, K^{com}, L^{com}, N^{com} , O^{com} and P^{com} using a combination of information from both the single-slice scans and SCTS.

5.3. Comparison of carcass and meat quality traits of divergent sheep genotypes and *In vivo* prediction of intramuscular fat content in the loins of divergent sheep genotypes using X-ray computed tomography

5.3.1. Genotype comparison of Chem_IMF and Pr_Cfat

After adjusting for CTLWT, Chem_IMF in the loin was significantly affected by genotype (*P* <0.001), with the highest levels in SBF, followed by TexX, then Tex (Table 5.8). Sex within genotype was also shown to have a significant effect on Chem_IMF, after adjusting for CTLWT, with females showing higher values than males.

Fitting the same model, but adjusting for Pr_Cfat rather than CTLWT, means for Chem_IMF still showed a significant genotype effect (*P* <0.001) and each genotype ranked similarly as with the previous model. Sex within genotype for both Tex and SBF was significant, however no significant effect of sex within genotype was shown in the TexX, where the males had been castrated (Genotype x Sex; Table 5.8).

After adjusting for CTLWT, the predicted means for Pr_Cfat show that there was a significant genotype effect on Pr_Cfat (*P* <0.001), with SBF lambs ranking highest and Tex lambs

ranking lowest. A significant sex effect was shown within genotype where females ranked significantly higher than males in all genotypes (P <0.05; Table 5.8)

Table 5.8: Adjusted least square means for the effects of genotype and genotype by sex interaction on Chem_IMF and Pr_Cfat. Standard error of the means (s.e) or standard errors of the difference between means (s.e.d) are shown.

Factor	Genotype					Genotype × Sex					
	Tex	SBF	TexX	s.e.d	*p* value	Tex		SBF		TexX	
						Male (s.e)	Female (s.e)	Male (s.e)	Female (s.e)	Male (s.e)	Female (s.e)
Chem_IMF*	1.51[a]	2.42[b]	1.90[c]	0.06	<0.001	1.23[a] (0.05)	1.77[b] (0.04)	2.12[a] (0.06)	2.72[b] (0.06)	1.81[a] (0.07)	1.99[b] (0.07)
Chem_IMF**	1.67[a]	2.20[b]	1.83[c]	0.05	<0.001	1.55[a] (0.04)	1.78[b] (0.04)	2.10[a] (0.05)	2.30[b] (0.05)	1.91[a] (0.06)	1.76[a] (0.06)
Pr_Cfat	2.44[a]	3.39[b]	2.81[c]	0.06	<0.001	2.04[a] (0.05)	2.83[b] (0.05)	2.87[a] (0.06)	3.89[b] (0.06)	2.39[a] (0.07)	3.22[b] (0.07)

*Model corrected for CTLW, **Model corrected for Pr_Cfat, Genotype means not sharing a common character in their superscript, within factor (same row), are significantly different ($p<0.05$), Genotype × Sex means not sharing a common character in their superscript, within genotype (same column) and within factor (same row), are significantly different ($p<0.05$)

Table 5.9: Validation of selected models across SBF and TexX data sets

	Texel	SBF	TexX
Model	Adj R^2 (RMSEP)	R^2 (RMSEP)	R^2 (RMSEP)
A	0.66 (0.40)	0.64 (0.49)	0.37* (0.48)
B	0.68 (0.39)	0.57* (0.54)	0.36* (0.49)

* Coefficient of determination (R^2) is significantly different from development data (Texel) ($P<0.05$)

5.3.2. Accuracy of prediction equations in SBF and TexX

Model A, derived using Tex data, which included information from CT predicted carcass fat (Pr_Cfat), average muscle density in the fifth lumbar vertebra scan (LV5MD) and average muscle density in the eighth thoracic vertebra scan (TV8MD), performed well when validated in the SBF data, resulting in $R^2 = 0.64$, but resulted in a significant reduction in the coefficient of determination (R^2) when validated using the TexX data ($R^2 = 0.37$; Table 5.9). Model B, also derived on Tex data, which included information from CT predicted carcass fat (Pr_Cfat), average soft tissue density in the fifth lumbar vertebra and eighth thoracic vertebra scans (LV5STD, TV8STD) and the standard deviation of soft tissue density in the ischium, fifth lumbar vertebra and eighth thoracic vertebra scans (ISCSTSD, LV5STSD, TV8STSD), explained a high proportion of the variance ($R^2= 0.68$) in the training data set (Tex), but explained significantly less variance when validated against both the SBF data and the TexX data ($R^2 = 0.57$ and 0.36 respectively, Table 5.9). Plots of the fitted values from both models (A and B) for all three data sets can be seen in Figure 5.1.

Because the Tex data were used to derive the prediction equations, the regression coefficients for both models are close to 1, as expected (Figure 5.1i). The slopes in Figure 5.1ii (SBF data) diverge from unity, model A; b = 1.49, P < 0.0001 and model B; b = 0.81, P < 0.0001. Both models produce a bias, with model A overestimating lower values and underestimating larger values, whilst model B overestimates across the range of values, with that overestimation increasing as values increase. The slopes in Figure 5.1iii (TexX data) also diverge from unity, model A; b = 0.78, P = 0.004 and model B; b = 0.53, P < 0.0001. Both models produce a bias with both model A and B underestimating lower values and overestimating higher values, however the bias appears to be greater in model B.

Plots of the residuals against Chem_IMF from both models (A and B) for all three data sets can be seen in Figure 5.2. The slopes for the residuals in the Tex data (Figure 5.2i) indicate that both models are overestimating smaller values and underestimating larger values and indicate a bias in the slope in both model A and B (b = -0.34, P<0.001 and b = -0.32, P<0.001 respectively). The slopes in Figure 5.2ii (SBF) indicate that both models overestimate smaller values and underestimating larger values and again indicate a bias in both model A and B (b = -0.57, P<0.001 and b = -0.29, P <0.001 respectively).The slopes for the residuals in the TexX data (Figure 5.2iii) indicate that both models are overestimating smaller values and underestimating larger values and once again indicate a bias in the models (A; b = -0.52, P<0.001 and B; b = -0.33, P<0.001).

(i)

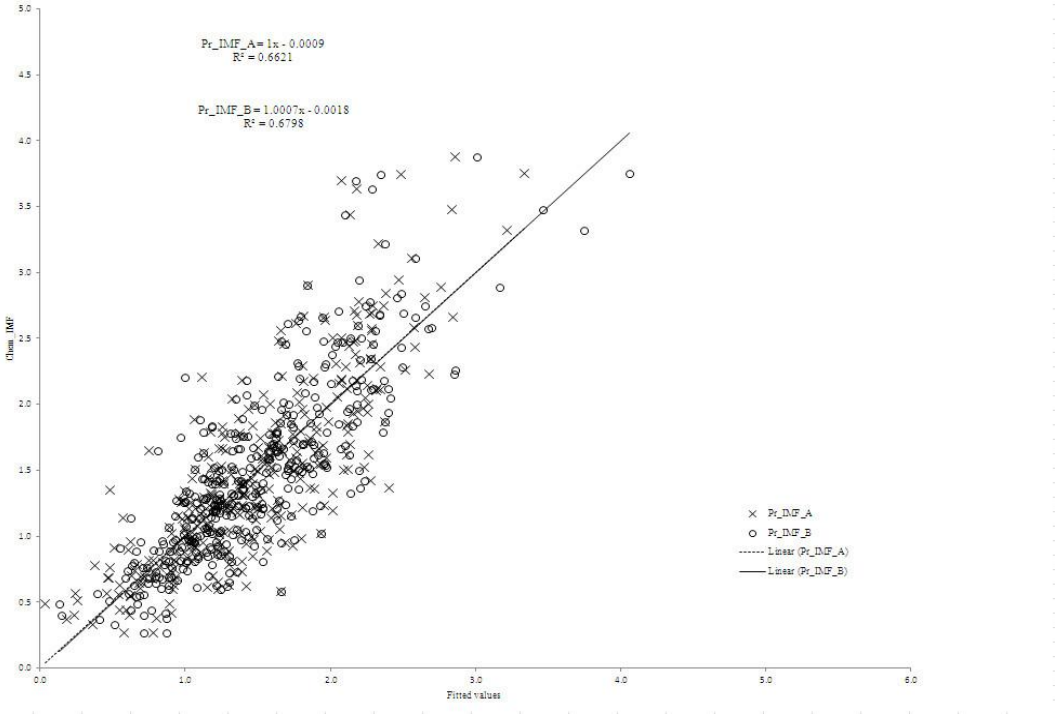
Pr_IMF_A= 1x - 0.0009
R² = 0.6621
Pr_IMF_B= 1.0007x - 0.0018
R² = 0.6798
Chem_IMF
Fitted values
Pr_IMF_A
Pr_IMF_B
Linear (Pr_IMF_A)
Linear (Pr_IMF_B)

(ii)

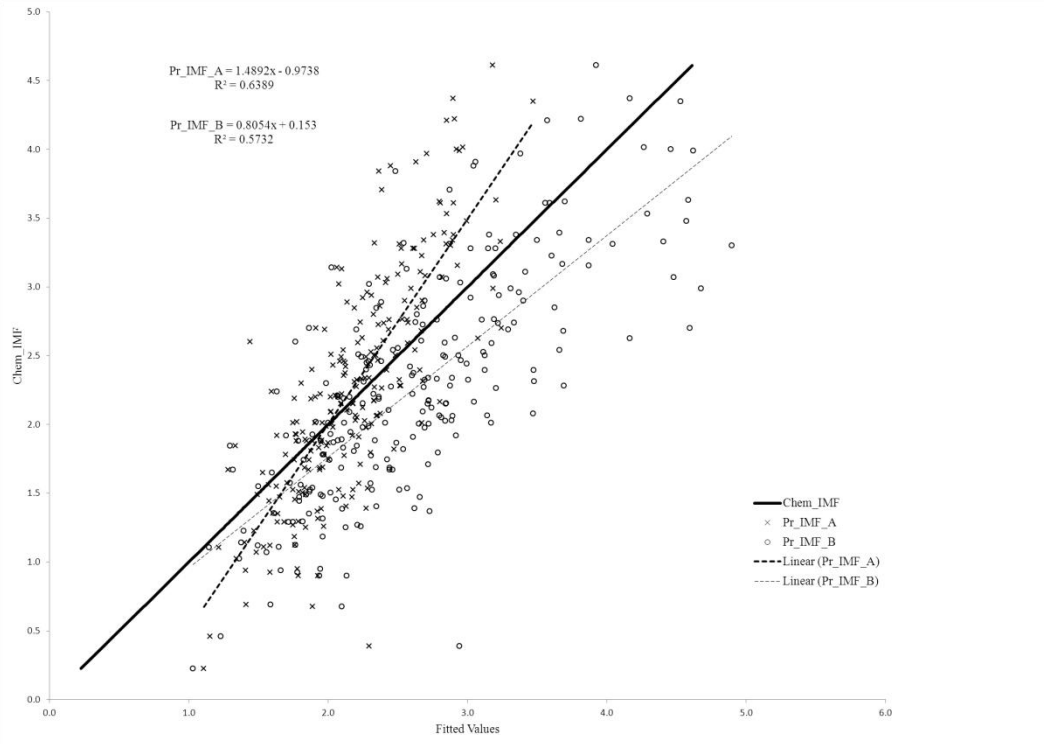
Pr_IMF_A = 1.4892x - 0.9738
R² = 0.6389
Pr_IMF_B = 0.8054x + 0.153
R² = 0.5732
Chem_IMF
Fitted Values
Chem_IMF
Pr_IMF_A
Pr_IMF_B
Linear (Pr_IMF_A)
Linear (Pr_IMF_B)

(iii)

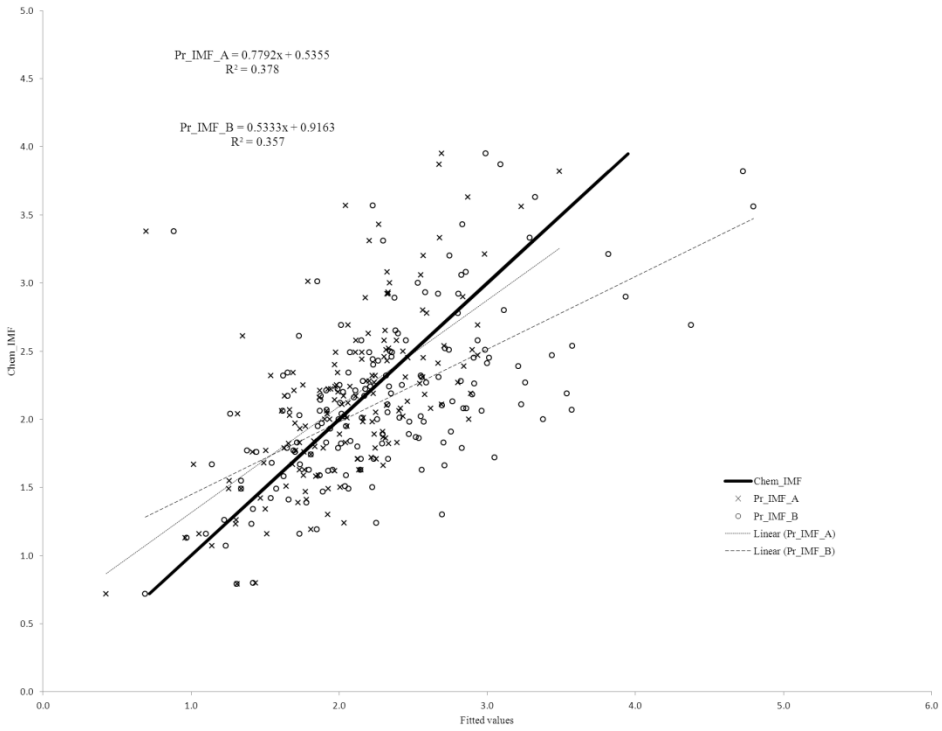

Figure 5.1 Fitted values of predicted IMF using both models (A and B) against Chem_IMF for the Tex development data (i), SBF data (ii) and the TexX data (iii)

(i)

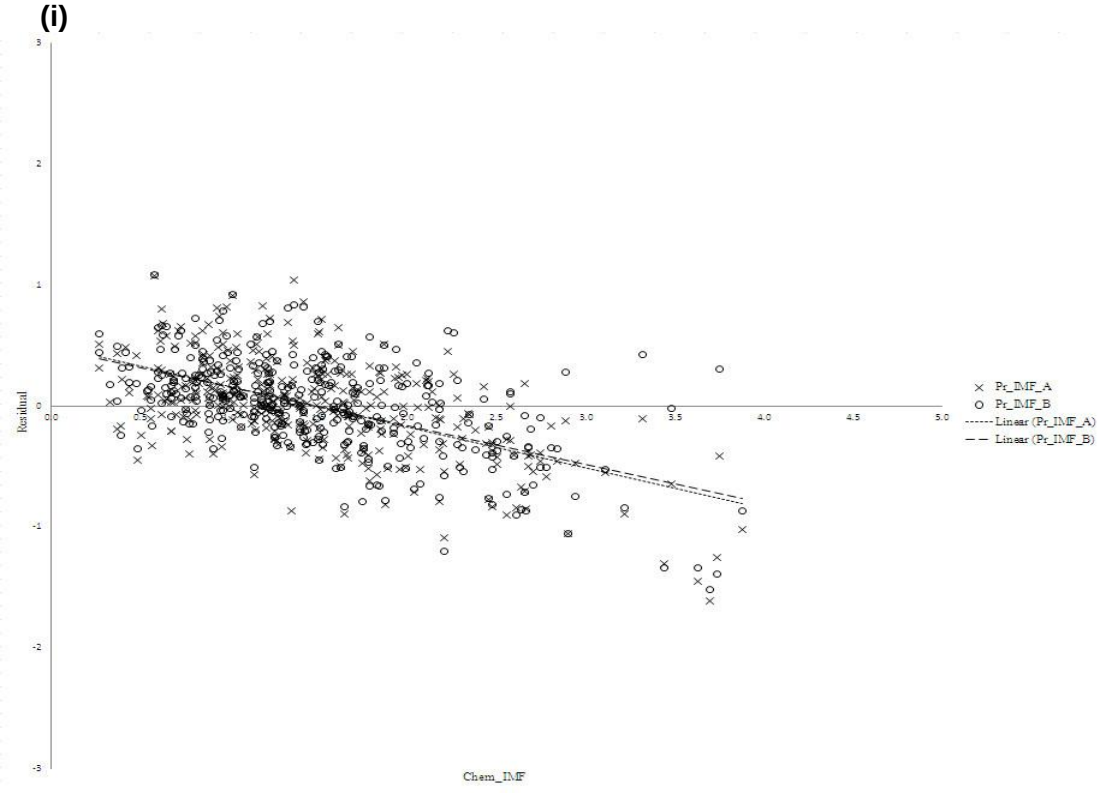

(ii)

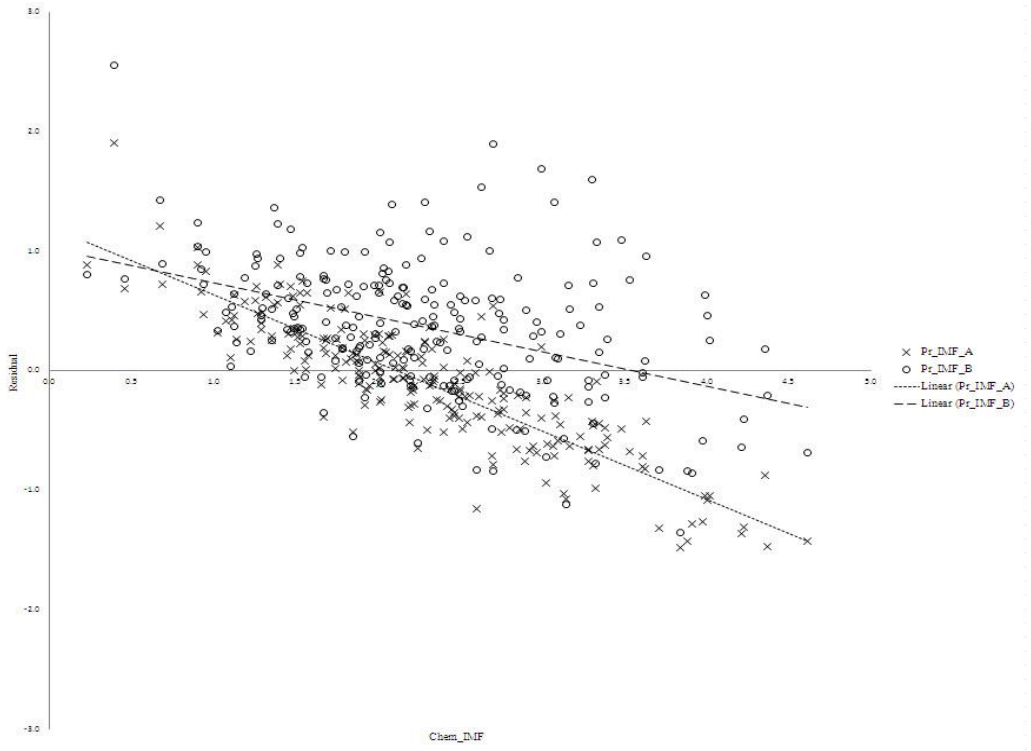

(iii)

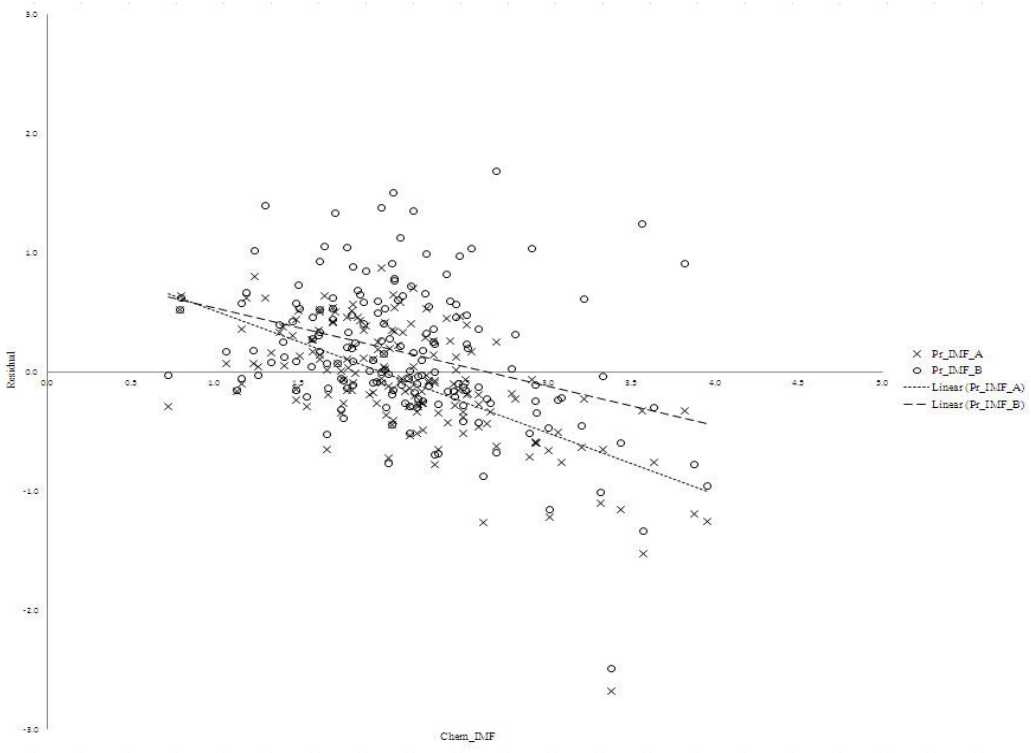

Figure 5.2 Residual values of predicted IMF using both models (A and B) against Chem_IMF for the Tex development data (i), SBF data (ii) and the TexX data (iii)

Table 5.10 compares the average absolute error of CT-predicted IMF in all three genotypes, as estimated by the two prediction equations, with Chem_IMF. Average absolute error is expressed as the mean of the error of prediction (residuals) expressed as IMF percentage, of the fitted values over Chem_IMF.

Model A performs better in both the SBF and TexX, with an average absolute error of 0.42 and 0.37 percentage points in SBF and TexX respectively and an average absolute error of 0.30 in the Tex data. Model B performs slightly better in the Tex data with an absolute error of 0.29, however in both the SBF and TexX data, model B has a slightly higher absolute error when compared to model A within the same genotype (SBF = 0.53, TexX = 0.45).

The phenotypic correlations between Chem_IMF and CT variables are presented in Table 5.11. This shows weaker phenotypic relationships between CT variables and Chem_IMF in the TexX data, compared to the other genotypes. However, although the strength of relationship differs across genotypes, the ranking remains similar. The exceptions are the relationship between age at CT and Chem_IMF and age at slaughter and Chem_IMF, where in the TexX data this relationship is positive, rather than negative as in the Tex and SBF data, however the relationship is very weak across all genotypes.

Table 5.10: Average absolute error, as the absolute mean of the magnitude of the residuals expressed as IMF percentage of the Pr_IMF (%) in both models (A and B) from Chem_IMF (%) in all three genotypes

Genotype	**Tex**	**SBF**	**TexX**
Model	Average absolute error	Average absolute error	Average absolute error
A	0.30	0.42	0.37
B	0.29	0.53	0.45

Table 5.11: Correlation (r) between Chem_IMF and CT traits employed in the prediction models within each data set

	Texel (n=370)	SBF (n=230)	TexX (165)
CTLWT	0.41	0.32	0.26
CTAGE	-0.14	-0.22	0.14
LV5MD	-0.71	-0.60	-0.46
TV8MD	-0.72	-0.56	-0.50
LV5STD	-0.76	-0.74	-0.58
TV8STD	-0.76	-0.73	-0.57
ISCSTSD	0.68	0.59	0.47
LV5STSD	0.65	0.68	0.52
TV8STSD	0.65	0.64	0.50
Pr_Cfat	0.71	0.74	0.54
SL_AGE	-0.11	-0.14	0.17
Model A	0.81	0.80	0.61
Model B	0.82	0.76	0.60

5.4. Preliminary genetic parameters of CT estimated traits and meat quality traits in Texel sheep

5.4.1. Animal model results

Estimates of additive genetic variance (V_A), residual variance (V_R), phenotypic variance (V_P) and heritability (h^2) estimates for the live weight traits, *post-mortem* meat quality traits and *in vivo* CT traits from the univariate analyses are shown in Table 5.12

Both models for CTLWT and chemical IMF failed to converge and were unable to produce estimates of the variance components or heritabilities. Very high heritabilities were estimated for SLWT, CTFW, PIMF1 and PIMF2 (0.88 to 0.98). The estimated heritability of ShF was very low (0.07) and not significantly different from zero with a S.E of 0.09.

Table 5.12: Estimated heritability's (S.E.) for the live weight, meat quality and computed tomography traits

Trait	CTLWT*	SLWT	ShF	IMF*	CTFW	PIMF1	PIMF2
V_A	21.18	23.50	0.13	0.33	1.01	0.27	0.23
V_R	0.00005	0.45	1.78	0.000001	0.05	0.01	0.03
V_P	21.18	23.94	1.91	0.33	1.06	0.28	0.26
h^2	1.00 (0.00)	0.98 (0.18)	0.07 (0.09)	1.00 (0.00)	0.95 (0.19)	0.95 (0.17)	0.88 (0.17)

*****Model not converged

Bivariate analyses were investigated using an animal model between the traits included in Table 4.5, with very little success (results not presented), producing unreasonable genetic parameters or non-convergence in all models.

The primary aim in these analyses was to estimate the genetic correlations between chemically extracted IMF measured *post-mortem*, and the CT predicted traits (PIMF1 and 2, CTFW), however these analyses were unsuccessful due to lack of convergence initially in the univariate model for one of the main traits of interest (IMF), although some univariate models did converge, and S.E were small in the estimates. The results were considered not to be accurate, given the unrealistically high h^2 estimates.

5.5. Genetic parameters for growth, carcass composition and intramuscular fat in Texel sheep measured by x-ray computed tomography and ultrasound

Significance of fixed effects and linear covariates fitted in the univariate analysis are presented in Table 5.13.

The means, standard deviations (SD) and coefficient of variation (CV) for the growth, US and CT traits used in the study are shown in Table 5.14. Mean intramuscular fat percentage as predicted by CT in PIMF1 and PIMF2 was 2.32% (SD 0.64) and 1.84% (SD 0.46) respectively, with a minimum of 0.62% and 0.26% respectively and a maximum of 5.12% and 3.60% respectively.

Table 5.13: Significance from the univariate analyses of fixed effects and covariates for each growth, US and CT trait analysed
Cov^1 = Age at US scanning, Cov^2 = Age at CT scanning
ns = non-significant, * = p<0.05, ** = p<0.01, *** = p<0.001

Trait group	Trait	Birth Type	Dam Age	Scanner	Flock	Year	Flock x Year	Cov^1	Cov^2
Live weight	8WWT	***	***		***	*	***		
	21WWT	***	***		***	*	***	***	
Ultrasound	USMD	***	ns		***	***	***	***	
	USFD	***	ns		***	***	***	***	
Computed Tomography	CTFW	***	**	***	***	***	***		***
	CTMW	***	**	**	***	ns	***		***
	CTmusc	**	ns	***	***	ns	***		***
	CTema	***	ns	*	***	ns	***		***
	PIMF1	***	**	***	***	**	***		***
	PIMF2	***	**	ns	***	ns	***		***

Table 5.14: Descriptive statistics for growth, ultrasound and computed tomography traits

Trait group	Trait	n	Mean	SD	Minimum	Maximum	CV (%)
Live weight	8WWT	1867	27.26	4.34	11.1	41.8	15.9
	21WWT	1959	56.46	8.39	26	90	14.9
Ultrasound	USFD	1957	3.01	1.39	0.4	9.5	46.4
	USMD	1957	32.7	3.38	20.3	43	10.4
Computed Tomography	CTFW	1971	5.19	1.67	1.26	11.57	32.2
	CTMW	1971	17.52	2.54	9.36	25.32	14.5
	CTmusc	1971	67.93	6.94	40	86	10.2
	CTema	1971	27.45	4.29	14.35	44.4	15.6
	PIMF1	1971	2.32	0.64	0.62	5.12	27.7
	PIMF2	1971	1.84	0.46	0.26	3.60	25.2

Table 5.15: Variances, phenotypic correlations and genetic parameters (S.E) for the growth, ultrasound and computed tomography traits

Trait	8WWT	21WWT	USFD	USMD	CTFW	CTMW	CTmusc	CTema	PIMF1	PIMF2
V_A	2.96	10.53	0.47	2.50	0.48	0.93	14.18	4.31	0.08	0.05
V_P	11.72	28.92	1.17	7.85	1.45	2.60	33.48	11.76	0.22	0.16
8WWT	**0.25 (0.07)**	0.57 (0.02)	0.13 (0.03)	0.19 (0.03)	0.48 (0.02)	0.51 (0.02)	0.13 (0.03)	0.29 (0.03)	0.40 (0.02)	0.26 (0.03)
21WWT	0.64 (0.11)	**0.36 (0.06)**	0.45 (0.02)	0.43 (0.02)	0.73 (0.01)	0.81 (0.01)	0.27 (0.03)	0.51 (0.02)	0.57 (0.02)	0.36 (0.02)
USFD	ns	0.42 (0.11)	**0.40 (0.07)**	ns	0.65 (0.02)	0.32 (0.03)	0.12 (0.03)	0.25 (0.03)	0.57 (0.02)	0.51 (0.02)
USMD	0.21 (0.18)	0.52 (0.12)	ns	**0.32 (0.07)**	0.37 (0.02)	0.50 (0.02)	0.27 (0.03)	0.66 (0.02)	0.21 (0.03)	0.12 (0.03)
CTFW	0.77 (0.12)	0.66 (0.08)	0.61 (0.09)	0.48 (0.13)	**0.33 (0.07)**	0.63 (0.02)	0.24 (0.03)	0.44 (0.02)	0.88 (0.01)	0.71 (0.01)
CTMW	0.43 (0.13)	0.76 (0.06)	0.15 (0.13)	0.59 (0.11)	0.49 (0.10)	**0.36 (0.06)**	0.33 (0.02)	0.69 (0.01)	0.43 (0.02)	0.21 (0.03)
CTmusc	0.20 (0.16)	0.44 (0.12)	ns	0.39 (0.12)	0.41 (0.13)	0.51 (0.11)	**0.42 (0.07)**	0.36 (0.02)	0.15 (0.03)	0.09 (0.03)
CTema	0.34 (0.16)	0.54 (0.10)	0.25 (0.14)	0.78 (0.08)	0.50 (0.12)	0.71 (0.07)	0.48 (0.11)	**0.37 (0.06)**	0.24 (0.03)	0.11 (0.03)
PIMF1	0.49 (0.15)	0.44 (0.11)	0.64 (0.10)	0.24 (0.15)	0.83 (0.04)	0.20 (0.13)	0.19 (0.14)	ns	**0.36 (0.07)**	0.90 (0.01)
PIMF2	0.24 (0.18)	ns	0.60 (0.11)	ns	0.59 (0.10)	ns	ns	ns	0.89 (0.03)	**0.31 (0.07)**

Heritabilities are in bold on the diagonal, genetic correlations below the diagonal and phenotypic correlations are above.

Correlations with S.E. greater than the correlation coefficient were not significantly different from zero (ns)

Estimates of variance components and heritability estimates for the growth and *in vivo* US and CT traits measured are shown in Table 5.15. Moderate heritabilities were estimated for growth traits tested in the study, with moderate to high heritabilities estimated for US and CT traits. Heritability estimates for the novel CT predicted IMF traits were moderate and similar: h^2 0.36 ± 0.07 for PIMF1 and h^2 0.31 ± 0.07 for PIMF2.

Estimates of genetic correlations amongst growth, US and CT traits, including the novel intramuscular fat estimations from CT, are shown in Table 5.15. Correlations from 0.1 to 0.3 were considered weak, from 0.4 to 0.6 moderate and correlations greater than 0.6 were considered as strong, correlations with a S.E. greater than the correlation coefficient were not significantly different from zero.

Strong positive genetic correlations were found between 8WWT and 21WWT (r_g 0.64 ± 0.11), and between 8WWT and CTFW (r_g 0.77 ±0.12). Genetic relationships between 21WWT and CTMW were also strong and positive (r_g 0.76 ± 0.06). Genetic relationships between US and CT carcass fat measurements (USFD, CTFW) were strong and positive (r_g 0.61 ± 0.09), and strong positive genetic correlations were estimated between USFD and PIMF1 and PIMF2 (r_g 0.64 and 0.60).

Genetic correlations between USMD and CTema were strong and positive (r_g 0.78 ± 0.08), while the relationship between USMD and CTMW was positive and moderate (r_g 0.59 ± 0.11).

A strong positive genetic correlation was found between CTFW and PIMF1 (r_g 0.83 ± 0.04), and a moderate positive correlation was found between CTFW and PIMF2 (r_g 0.59 ± 0.10). The genetic correlations between PIMF1 and the remaining current index traits (8WWT, USMD, USFD, CTMW, CTmusc) are low to moderate ranging from r_g 0.19 to 0.64 and stronger than the correlations seen between the same index traits and PIMF2 which were only significant in 8WWT (r_g 0.24 ± 0.18) and USFD (r_g 0.60 ± 0.11) (Table 5.15), with the muscularity traits (CTMW and CTmusc) not significantly correlated with PIMF2. The genetic correlation between PIMF1 and PIMF2 was strong and positive (r_g 0.89 ± 0.03).

Phenotypic correlation estimates among the growth, US and CT traits were consistent with the direction and magnitude of the corresponding genetic correlations (Table 5.15). Strong phenotypic correlations were found for pairings of traits with strong genetic correlations and generally the phenotypic correlations were smaller than the corresponding genetic correlation estimates.

6. General Discussion

6.1. CT as a method for estimating MQ traits in Texel sheep

Computed tomography has been used in UK terminal sire sheep breeding programmes for the last few decades, with elite rams from several terminal sire breeds (e.g. Texel, Suffolk and Charollais) now routinely scanned. Carcass fat and lean weight can be predicted with very high accuracy (98-99%) using CT (even just using the Reference scan method), and in order to increase the viability and value of CT scanning selection programmes, novel and economically important CT based phenotypes, should be included in current two-stage selection programmes. Such novel phenotypes include MQ traits such as IMF and shear-force. The current factors affecting the lamb carcass price are carcass weight, conformation and carcass fatness, thus systems aiming to produce high quality carcasses have currently focussed on these economically important traits. The consideration of MQ factors (e.g. shear-force and IMF) has until now been limited to the measurement of such traits *post-mortem,* which is time-consuming, expensive and destructive, and in turn limits the inclusion of these traits into current selection programmes. It has been shown that CT provides an opportunity to overcome these previous limitations in some MQ traits and to obtain these measures on live animals, the selection candidates.

6.1.1. Shear-force

Throughout the study, CT predictors did not explain much of the variance in shear-force, with a maximum Adj R^2 of 0.14 (RMSEP = 0.15) using information from routine reference scan images and no significant improvement was seen when spiral CT scan images were used. This objective MQ trait is understandably easily related to organoleptic traits such as tenderness by the consumer, and would be easily marketable as a 'proxy' trait for eating quality in live lambs. However the lack of accuracy achieved in this project and elsewhere does not provide sufficient confidence in the ability of CT to predict shear-force.

The inability of *in vivo* CT to predict the *post-mortem* trait shear-force may be due to the chemical and compositional changes that occur during the processing, cooking and ageing of a sample of meat (in this case lamb loin). These chemical and compositional changes include cooking loss, ultimate pH, drip loss, and *post mortem* glycolysis. Factors that also have an effect on shear-force can be muscle fibre type and size, and clearly the connective tissue content. All these factors contribute to the ultimate values of shear-force and chemical and compositional changes mean that muscle *post-mortem* is far removed from the same skeletal muscle *in-vivo*. Mechanically measured shear-force is also known to have low

repeatability which may also partially explain the low predictability. CT was unable to predict such a 'tangible' trait *in-vivo*, however with further work it may be possible to develop a method and increase the accuracy of predicting such *post-mortem* traits in primal cuts or retail cuts using CT of the meat cuts themselves (rather than live animal CT) and multi-object image analysis which would reduce the cost of CT scanning individual cuts by allowing several objects to be scanned and analysed simultaneously.

6.1.2. Intramuscular fat

Following a review of the literature by Savell and Cross, (1988) a minimum level of 3% IMF in grilled cuts of red meat such as beef and lamb was recommended to ensure consumer acceptability in terms of eating quality, with some studies recommending as high as 5% (Hopkins et al., 2006) in lamb meat, which we may define as a minimum 'window' of acceptability ranging from 3-5% IMF in lamb. Although it should be noted that a current and comprehensive study on the relationship between IMF in lamb and consumer taste panel results in the UK has yet to be completed (Lambe et al., 2017) and previous studies have highlighted country differences in preferences of lamb meat (Sanudo et al., 1998).

This study provides evidence that in both the experimental animals included in chapter two and the commercial animals included in chapter six, the average levels of IMF within both populations falls well below these recommended levels for optimal eating quality. These initial findings reinforce the requirement for increased attention to levels of IMF in the production of lamb meat in the UK. This is of course restricted by current methods of determining IMF levels *post-mortem*. However both chapters two and three have provided evidence of the ability of CT to predict with high accuracy IMF content in the loin of Texel sheep *in-vivo*. The methods used during the analyses were intended to be thorough in the process of including a large number of possible combinations of CT measures available, alternative image processing, and also using both two-dimensional, three-dimensional and a combination of these CT methods. This approach succeeded in identifying optimum prediction equations balanced for accuracy and practical application amongst all possible combinations of CT measures and methods, providing robust and accurate estimations of IMF content in Texel lamb loins. Throughout the study, it was considered that, the use of CT predicted IMF, where the prediction included total carcass fat, may complicate the divergent genetic selection for increased IMF against a reduction in carcass fatness. Therefore the work attempted to build and use prediction models with a higher independence from CT predicted carcass fatness. To address this, prediction models were developed both including and excluding related measures of total carcass fatness and the method of virtual dissection has been used.

The results from chapters two and three identified several possible prediction models for IMF producing prediction accuracies ranging from 63% - 71%, greatly improving on accuracies reported in previous studies ranging from R^2 0.36 – 0.57 (Karamichou et al., 2006; Macfarlane et al., 2006; Lambe et al., 2010b). No significant improvement was made on the accuracies achieved from virtual dissection, the use of three-dimensional CT measures or the combination of both two-dimensional and three-dimensional CT measures. The selection of optimal models was based on the use of CT information from current commercial CT methods using two-dimensional CT measures from three available reference scan images, three-dimensional spiral CT information and a combination of two-dimensional and three-dimensional. For the reasons previously highlighted, two optimal models were chosen; one including and another excluding CT predicted total carcass fat weight. As we know that there is a scanner effect on density values within soft tissue ranges between different scanners (Bunger et al., 2008), and two different scanner types were used between farms in both the experimental and commercial scanning procedures, scanner-specific equations were developed. Two models were ultimately selected from the work carried out in chapters two and three.

6.1.3. Breed and sex effects on IMF and the application of CT predicted IMF models in different breed types

The prediction equations developed in chapter two on Texel sheep were applied across divergent breed types for which CT and chemical IMF data were available (Texel, Scottish Blackface and Texel cross Scotch Mule), the purpose of which was to investigate the accuracy of transferring CT prediction models developed on one particular breed type to other breed types. The IMF levels across the breed types and sexes were also compared.

The Texel population included in the study were significantly lower in both IMF and CT predicted carcass fat than Scottish Blackface and Texel cross Mule sheep. In the same animals this has translated to increased tenderness, stronger lamb flavour and higher overall liking in the Scottish Blackface when compared to the Texel lamb meat (Navajas et al., 2008), further affirming the effect IMF levels play in the perception of organoleptic traits such as tenderness, flavour and overall liking. Scottish Blackface lambs were on average highest in both carcass fat and IMF, followed by Texel cross Mule and finally Texel. Again this highlights the effect of breeding strategies focussed on increasing lean meat production while maintaining or reducing overall carcass fatness in terminal sire breeds when compared to breeds which do not focus so much on the terminal traits e.g. Scottish Blackface. That is not to suggest that the inclusion of CT MQ and carcass traits in maternal and crossbreeding

selection programmes would not be of interest (Conington et al., 2006) and the study provides evidence that CT predicted IMF may be assessed in Scottish Blackface.

Males on average were leaner across all breeds when compared at the same liveweight, which agrees with several studies reporting that entire males are on average the leanest, followed by castrates and females (Bass et al., 1990; Butler-Hogg et al., 1984; Dransfield et al., 1990; Kirton et al., 1982). In this study, entire males also showed lower levels of IMF at the same levels of carcass fatness than females, which were not observed in the Texel cross Mule lambs which were castrated and were shown to have similar mean levels of IMF to their female counterparts.

It was expected, that given the breed relationship between Texel and Texel cross Mule, the prediction equations would transfer across better than to the Scottish Blackface. However, it was the opposite, prediction accuracies in the Scottish Blackface data ranged from R^2 0.57 – 0.64 (RMSEP 0.49 – 0.54) and in the Texel cross Mule data accuracies ranged from R^2 0.36 – 0.37 (RMSEP 0.48 – 0.49). To investigate the differences in transferability across the breeds, obvious differences in the summary statistics were highlighted, with differences in age at CT and age at slaughter identified across the breed types. The further investigation of these age related differences and their effect on transferability, provided evidence that there was no effect of age either at CT or slaughter on the prediction accuracies. Furthermore, a breed specific approach was also taken to the Texel cross Mule dataset, producing breed specific coefficients. This also resulted in no improvements of accuracies. It was shown that there are some differences in the relationship between IMF and CT variables across the breed types / populations, which may explain the reduction in accuracies of prediction equations developed in Texel across to the Texel cross Mule. It should also be acknowledged that the structure, design and the experimental procedures of the experiments providing the data was not optimal for a definitive and comprehensive breed comparison for both IMF levels and the prediction equations. A structured study balancing fixed effects such as sex, breed type and random effects such as age at CT, age at slaughter, management regime etc. would be recommended to produce thorough, definitive and comprehensive results. These results are indicative of the transferability of the prediction equations developed in chapter two, however it would be recommended, that if these prediction equations were to be considered in other breed types, validation studies should be conducted to confirm the accuracies achieved.

6.1.4. Genetic parameters of ultrasound, CT estimated and meat quality traits in Texel sheep

There were ultimately two parts to the genetic analysis in the study, firstly the estimation of genetic parameters using the same, size-limited research data set as used in chapters two through to four, and secondly the use of a larger, more powerful dataset comprising historical commercial data held within the BASCO database. The initial genetic analyses using the research data had the aim to produce genetic relationships between *post-mortem* meat quality measurements such as shearforce and IMF and CT estimated traits including the novel CT predicted IMF traits. It was discovered that a combination of small animal numbers, and the design and research objective of the study to produce some of the data, resulted in a pedigree structure that limits the effectiveness of the research data set for genetic parameter estimation, this was as a result of both males and females being intensively selected in order to increase the genetic frequency of a QTL that was of interest for that original study. Closely related individuals in part of the study were used as parents and the common sires could be traced back to a single sire. Therefore, the aims of the initial genetic analysis were very difficult to achieve and results reported were seemingly unreasonable with regards to magnitude and /or accompanied by very large standard errors. The primary interest in this chapter was the quantification of the genetic basis and relationships between *post-mortem*, laboratory measured traits, with *in-vivo* meat and carcass quality traits. This remains a valuable relationship to understand and would require large numbers of animals, including pedigree information, CT data and laboratory measured MQ traits to achieve this. The CT methods of IMF prediction developed in this study may serve to enable the robust genetic analysis of these traits in future research or commercial studies.

Robust and accurate heritability estimates of the novel CT predicted IMF traits and genetic correlations with existing index traits were the main focus of the analysis using the commercial data set, alongside the confirmation of genetic parameters of current US, CT and growth traits, in order to enable the inclusion of CT predicted IMF into current breeding programmes. A larger industry data set was made available from the BASCO database, making it possible to estimate genetic parameters of these economically important traits with sufficient statistical power. Moderate heritabilities were estimated for growth traits, with moderate to high heritabilities estimated for US and CT traits. Heritability estimates for the novel CT predicted IMF traits were moderate (h^2 0.31-0.36) and strong positive genetic correlations were estimated between US measured fat depth and CT predicted IMF (r_g 0.60-0.64). Of particular interest was the genetic relationship between CT predicted fat weight and CT predicted IMF using each of the two models: which was found to be strong and positive

for the model inclusive of CT predicted carcass fat weight (r_g 0.83) and moderately positive for the model entirely independent of CT carcass fat measures (r_g 0.59). The genetic relationship between the two CT predicted IMF traits were strong and positive (r_g 0.89).

The heritability estimates for CT predicted IMF produced were similar to those for chemically extracted IMF found in previous studies (h^2 0.32-0.48; Karamichou et al., 2006; Lorentzen and Vangen, 2012; Mortimer et al., 2014). The similarity between heritabilities for CT predicted IMF and IMF is an indication of the prediction accuracy of CT predicted IMF *in-vivo* in Texel sheep. It is also apparent that both models are partially under different genetic control from CT carcass fatness. However the model not inclusive of CT carcass fat measures was less genetically correlated to CT carcass fat than the model inclusive of these measures. This provides evidence that a model for prediction of IMF that is not using carcass fat as a predictor can provide a similar accuracy as a model that uses CT carcass fat measures. Any selection scheme using CT to improve or maintain IMF and to reduce further carcass fat, works against the positive genetic correlation between the two fat depots. An IMF prediction model that is not using the information on carcass fat as predictor should be very valuable in such an approach aiming to identify "correlation breakers" as selection candidates, given that there is a large amount of variation in both fat depots (carcass fat and CT predicted IMF) in the commercial population used here (Figure 6.1).

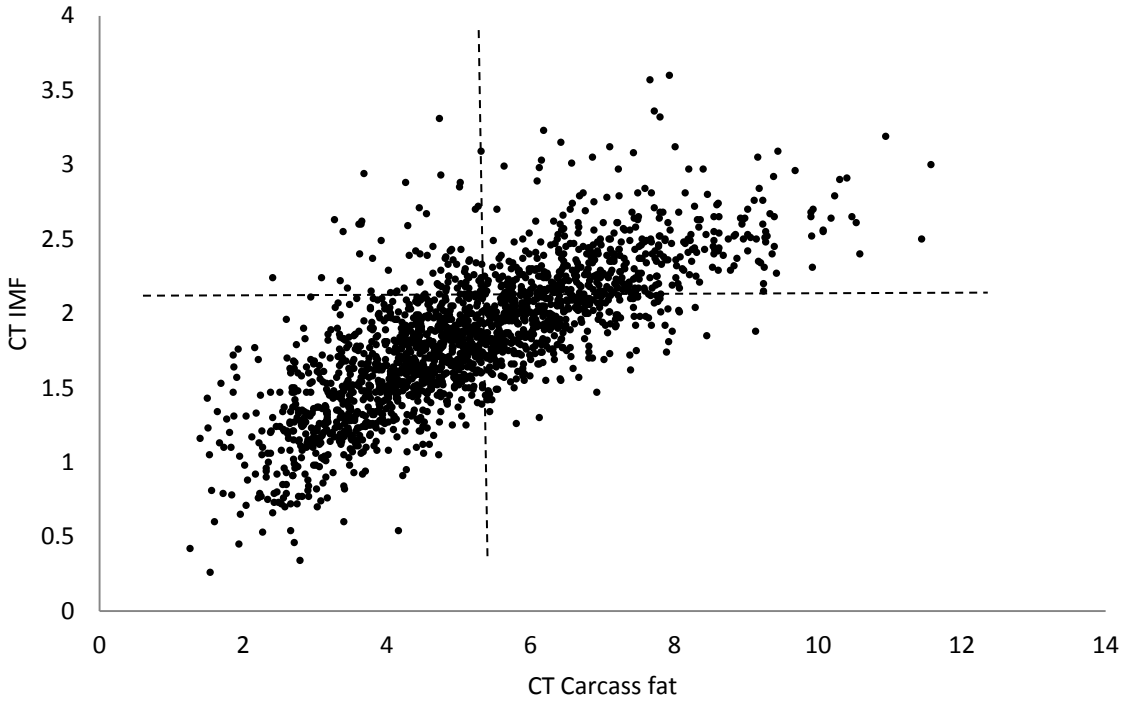

Figure 6.1: Plot of selection candidates from commercial CT data based on CT predicted carcass fat and CT predicted IMF using model PIMF2 (n=1971, r = 0.76)

There may already be potential selection candidates within the commercial population which fit the criteria for lean carcasses at optimal levels of IMF, such as those within the top left quadrant in Figure 6.1. It can be concluded that CT provides a highly accurate tool to identify these selection candidates.

Currently the Texel breeding programme's multi-trait selection index focuses mainly on increased US muscle depth, CT muscle weight and a very slight reduction of CT carcass fat weight. Estimated breeding values for IMF should be immediately introduced into current breeding programmes for Texel sheep and in the future other breeds. Given that the Texel breed is already very lean in comparison to some other breeds as discussed previously, the inclusion of CT predicted IMF into the existing multi-trait selection index would enable breeders to maintain the lean and muscular attributes of the breed whilst selecting for increased IMF levels which are closer to the levels recommended for optimal eating quality, providing the industry with an improved balance of economically important carcass quality traits in the abattoir alongside optimal eating quality characteristics for the consumer.

It is of note in this context, that future value based payments systems in abattoirs will probably reward farmers for meat quality and the time unit of breeding is generations not weeks or months. In other words, such an approach would make the industry more future proof.

6.1.5. Future work

Further steps to achieve the integration of these CT predicted IMF methods into current two-stage selection practices and routine genetic evaluations would require the addition of CT predicted IMF into current commercial analyses of CT images alongside the integration of CT predicted IMF into current multi-trait selection indices and the existing two-stage selection programmes for Texel sheep. The investigation and further development of CT predicted IMF methods in other terminal and maternal breeds should be continued and will lead to additional benefits of CT to the entire UK sheep breeding industry.

One area of potential further research related to the eating quality of lamb, is the prediction of eating quality in primal or retail cuts of meat. Very high accuracies have been achieved in beef primal cuts (Prieto et al., 2010) but not yet in lamb loins (Lambe et al., 2017). However a more structured and thorough analyses of several types of cuts, including primal cuts such as the entire saddle, gigot and shoulder of lamb down to rib joints and fully dissected loins may be more successful in the quantification of meat eating quality traits in lamb from CT scanning meat cuts.

The current study also concentrated on the most valuable cut of the loin, and the correlation between the measurement of IMF and in relation, eating quality, between the loin and other commercially important muscles (i.e. shoulder, rump etc.) might be investigated.

These suggested subsequent studies should also further investigate the effect of in vivo CT scanning vs. *post mortem* with the latter possibly affected by chilling or even freezing and thawing.

7. Reference List

Allen, N. 2010. The Outlook and Opportunities for the English Sheep Industry 2010 and Beyond.

Bass, P. D., J. A. Scanga, P. L. Chapman, G. C. Smith, J. D. Tatum, and K. E. Belk. 2008. Recovering value from beef carcasses classified as dark cutters by United States Department of Agriculture graders. J. Anim. Sci. 86:1658–1668.

Bunger, L., C. A. Glasbey, J. K. Brown, J. M. MacFarlane, K. A. McLean, and N. L. Lambe. 2008. Effects of different scanners in Computer tomography. In: Proceedings of the Farm Animal Imaging Congress. Rennes, France. p. 1–3.

Bunger, L., and W. G. Hill. 2005. Genetics of body composition and metabolic rate. In: E. J. Eisen, editor. The Mouse in Animal Genetics and Breeding Research. Imperial College Press, London. p. 131–160.

Bünger, L., J. M. Macfarlane, N. R. Lambe, J. Conington, K. A. McLean, K. Moore, and C. A. Glasbey. 2011. Use of X-ray computed tomography (CT) in UK sheep production and breeding L. Bünger; J.M. Macfarlane, N. R. Lambe, J. Conington, K. A. McLean, K. Moore, C.A. Glasbey. In: S. Karuppasamy, editor. CT Scanning - Techniques and Applications. INTECH Open access Publisher. p. 329–348.

Conington, J., N. Lambe, L. Bünger, K. McLean, S. C. Bishop, and G. Simm. 2006. Evaluation of responses to multi-trait selection indexes and genetic parameters for Computer Tomography-derived carcass traits in UK hill sheep. Proc. 8th World Congr. Genet. Appl. to Livest. Prod. Belo Horizonte, Minas Gerais, Brazil, 13-18 August, 2006:4–19.

Fernandez, X., G. Monin, A. Talmant, J. Mourot, and B. Lebret. 1999. Influence of intramuscular fat content on the quality of pig meat — 2. Consumer acceptability of m. longissimus lumborum. Meat Sci. 53:67–72. Available from: http://www.sciencedirect.com/science/article/pii/S0309174099000388

Gerbens, F., A. J. M. Van Erp, F. L. Harders, F. J. Verburg, T. H. E. Meuwissen, J. H. Veerkamp, and M. F. W. Pas. 1999. Effect of Genetic Variants of the Heart Fatty Acid-Binding Protein Gene on Intramuscular Fat and Performance Traits in Pigs. J. Anim. Sci. 77:846–852.

Gilmour, a R., B. J. Gogel, B. R. Cullis, and R. Thompson. 2009. ASReml user guide. VSN International LTD.

Glasbey, C., and M. J. Young. 2002. Maximum a psteriori estimation of image boundaries by dynamic programming. Appl. Stat. 51:209–221.

Hopkins, D. L., R. S. Hegarty, P. J. Walker, and D. W. Pethick. 2006. Relationship between animal age, intramuscular fat, cooking loss, pH, shear force and eating quality of aged meat from sheep. Aust. J. Exp. Agric. 46:879–884.

Jones, H., R. Lewis, M. Young, and G. Simm. 2002. Incorporating CT measures of composition and muscularity into selection programs for Suffolk sheep. 7th World Congr. Genet. Appl. to Livest. Prod.:3–6. Available from: http://www.cabdirect.org/abstracts/20033053225.html

Jopson, N. B., P. R. Amer, and J. C. McEwan. 2004. Comparison of two-stage selection breeding programmes for terminal sire sheep. Proc. New Zeal. Soc. Anim. Prod. 64:212–216.

Karamichou, E., R. I. Richardson, G. R. Nute, K. A. McLean, and S. C. Bishop. 2006. Genetic analyses of carcass composition, as assessed by X-ray computer tomography, and meat quality traits in Scottish Blackface sheep. Anim. Sci. 82:151–162.

Karamichou, E., R. I. Richardson, G. R. Nute, J. D. Wood, and S. C. Bishop. 2007. Genetic analyses of sensory characteristics and relationships with fatty acid composition in the meat from Scottish Blackface lambs. Animal 1:1524–1531. Available from: http://journals.cambridge.org/action/displayAbstract?fromPage=online&aid=1422308&fulltextType=RA&fileId=S1751731107000754

Killinger, K. M., C. R. Calkins, W. J. Umberger, D. M. Feuz, and K. M. Eskridge. 2004. Consumer sensory acceptance and value for beef steaks of similar tenderness, but differing in marbling level. J. Anim. Sci. 82:3294–3301.

Kvame, T., and O. Vangen. 2007. Selection for lean weight based on ultrasound and CT in a meat line of sheep. Livest. Sci. 106:232–242.

Lambe, N. R., J. M. Macfarlane, R. I. Richardson, O. Matika, W. Haresign, and L. Bünger. 2010a. The effect of the Texel muscling QTL (TM-QTL) on meat quality traits in crossbred lambs. Meat Sci. 85:684–690. Available from: http://dx.doi.org/10.1016/j.meatsci.2010.03.025

Lambe, N. R., K. A. McLean, J. Gordon, D. Evans, N. Clelland, and L. Bunger. 2017. Prediction of intramuscular fat content using CT scanning of packaged lamb cuts and

relationships with meat eating quality. Meat Sci. 123:112–119. Available from: http://dx.doi.org/10.1016/j.meatsci.2016.09.008

Lambe, N. R., K. A. McLean, J. M. Macfarlane, P. L. Johnson, N. B. Jopson, W. Haresign, R. I. Richardson, and L. Bunger. 2010b. Predicting intramuscular fat content of lamb loin fillets using CT scanning. :9–10.

Lambe, N. R., E. A. Navajas, C. P. Schofield, A. V. Fisher, G. Simm, R. Roehe, and L. Bünger. 2008. The use of various live animal measurements to predict carcass and meat quality in two divergent lamb breeds. Meat Sci. 80:1138–1149.

Lewis, R. M., and G. Simm. 2002. Small ruminant breeding programmes for meat: progress and prospects. In: 7th World Congress of Genetics Applied to Livestock Production.

Lorentzen, T. K., and O. Vangen. 2012. Genetic and phenotypic analysis of meat quality traits in lamb and correlations to carcass composition. Livest. Sci. 143:201–209. Available from: http://dx.doi.org/10.1016/j.livsci.2011.09.016

Macfarlane, J. M., R. M. Lewis, G. C. Emmans, M. J. Young, and G. Simm. 2006. Predicting carcass composition of terminal sire sheep using X-ray computed tomography. Anim. Sci. Then Penicuik- 82:289. Available from: http://journals.cambridge.org/action/displayAbstract?fromPage=online&aid=779276%5Cnhttp://journals.cambridge.org/action/displayFulltext?pageCode=100101&type=1&fid=779288&jid=ASC&volumeId=82&issueId=03&aid=779276%5Cnhttp://www.bsas.org.uk/Publications/Anim

Mortimer, S. I., J. H. J. van der Werf, R. H. Jacob, D. L. Hopkins, L. Pannier, K. L. Pearce, G. E. Gardner, R. D. Warner, G. H. Geesink, J. E. Hocking Edwards, E. N. Ponnampalam, A. J. Ball, A. R. Gilmour, and D. W. Pethick. 2014. Genetic parameters for meat quality traits of Australian lamb meat. Meat Sci. 96:1016–1024. Available from: http://dx.doi.org/10.1016/j.meatsci.2013.09.007

Mudholkar, G. S. 2006. Fisher's Z-Transformation. In: Encyclopedia of Statistical Sciences. John Wiley & Sons, Inc.

Navajas, E. A., C. A. Glasbey, K. A. McLean, A. V. Fisher, A. J. L. Charteris, N. R. Lambe, L. Bunger, and G. Simm. 2006. In vivo measurements of muscle volume by automatic image analysis of spiral computed tomography scans. J. Anim. Sci. 82:545–553. Available from: http://journals.cambridge.org/production/action/cjoGetFulltext?fulltextid=779188%5Cnhttp://journals.cambridge.org/action/displayFulltext?type=1&fid=779188&jid=ASC&volumeId=82&is

sueId=04&aid=779176

Navajas, E. A., N. R. Lambe, A. V. Fisher, G. R. Nute, L. Bünger, and G. Simm. 2008. Muscularity and eating quality of lambs: Effects of breed, sex and selection of sires using muscularity measurements by computed tomography. Meat Sci. 79:105–112.

Pannier, L., D. W. Pethick, G. H. Geesink, A. J. Ball, R. H. Jacob, and G. E. Gardner. 2014. Intramuscular fat in the longissimus muscle is reduced in lambs from sires selected for leanness. Meat Sci. 96:1068–1075. Available from: http://dx.doi.org/10.1016/j.meatsci.2013.06.014

Payne, R., D. Murray, S. Harding, D. Baird, and D. Soutar. 2011. Introduction to GenStat for Windows. 14th ed. VSN International.

Prieto, N., E. A. Navajas, R. I. Richardson, D. W. Ross, J. J. Hyslop, G. Simm, and R. Roehe. 2010. Predicting beef cuts composition, fatty acids and meat quality characteristics by spiral computed tomography. Meat Sci. 86:770–779. Available from: http://dx.doi.org/10.1016/j.meatsci.2010.06.020

Sanudo, C., G. R. Nute, M. M. Campo, G. Maria, A. Baker, I. Sierra, M. E. Enser, and J. D. Wood. 1998. Assessment of commercial lamb meat quality by British and Spanish taste panels. Meat Sci. 48:91. Available from: http://www.sciencedirect.com/science/article/B6T9G-3S3N14F-9/2/75b06bd3c18f93bd3aa93729204cce94

Savell, J. W., and H. R. Cross. 1988. The role of fat in the palatability of beef, pork, and lamb. In: Designing Foods: Animal Product Options in the Marketplace. The National Academy of Sciences. p. 345–355.

Simm, G., R. M. Lewis, B. Grundy, and W. S. Dingwall. 2002. Responses to selection for lean growth in sheep. Anim. Sci. 74:39–50.

Snee, R. D. 1977. Validation of Regression Models: Methods and Examples. Technometrics 19:415–428. Available from: http://www.tandfonline.com/doi/abs/10.1080/00401706.1977.10489581

Sonesson, A. K., K. H. de Greef, and T. H. E. Meuwissen. 1998. Genetic parameters and trends of meat quality, carcass composition and performance traits in two selected lines of large white pigs. Livest. Prod. Sci. 57:23–32. Available from: http://www.sciencedirect.com/science/article/pii/S030162269800163 8%5Cnhttp://www.scien

cedirect.com/science/article/pii/S0301622698001638/pdfft?md5=b6d0ad7a450405efacf226e0b2f29605&pid=1-s2.0-S0301622698001638-main.pdf

Teye, G. A., P. R. Sheard, F. M. Whittington, G. R. Nute, A. Stewart, and J. D. Wood. 2006. Influence of dietary oils and protein level on pork quality. 1. Effects on muscle fatty acid composition, carcass, meat and eating quality. Meat Sci. 73:157–165.

Volodkevich, N. N. 1938. Apparatus for measurement of chewing resistance or tenderness of foodstuffs. J. Food Sci. 3:221–225. Available from: http://dx.doi.org/10.1111/j.1365-2621.1938.tb17056.x

Young, M. J., G. Simm, and C. A. Glasbey. 2001. Computerised tomography for carcass analysis. Proc. Br. Soc. Anim. Sci.:250–254.